Idaho National Engineering and Environmental Laboratory

INEEL/EXT-98-00820
Revision 2

July 1999

SCDAP/RELAP5 Modeling Of Heat Transfer And Flow Losses In Lower Head Porous Debris

L. J. Siefken
E. W. Coryell
S. Paik
H. Kuo

LOCKHEED MARTIN

INEEL/EXT-98-00820
Rev. 2

SCDAP/RELAP5 Modeling of Heat Transfer and Flow Losses in Lower Head Porous Debris

L. J. Siefken
E. W. Coryell
S. Paik
H. Kuo

Idaho National Engineering Laboratory
Lockheed Martin Idaho Technologies Company
Idaho Falls, Idaho 83415

Prepared for the
U.S. Nuclear Regulatory Commission
Washington, D. C. 20555

Abstract

Designs are described for models to calculate the heat transfer and flow losses in porous debris in the lower head of a reactor vessel. The COUPLE model in SCDAP/RELAP5 represents both the porous and nonporous debris that results from core material slumping into the lower head. Previously, the COUPLE model had the capability to model convective and radiative heat transfer from the surfaces of nonporous debris in a detailed manner and to model only in a simplistic manner the heat transfer from porous debris. In order to advance beyond the simplistic modeling for porous debris, designs were developed for detailed calculations of heat transfer and flow losses in porous debris. Correlations were identified for calculating convective heat transfer in porous debris for the following modes of heat transfer; (1) forced convection to liquid, (2) forced convection to gas, (3) nucleate boiling, (4) transition boiling, (5) film boiling, and (6) transition from film boiling to convection to vapor. Interphase heat transfer is modeled in an approximate manner. Correlations were identified for calculating the flow losses and interphase drag of fluid flowing through the interstices of the porous debris. These calculations for flow loss and interphase drag were integrated into the momentum equations in the RELAP5 part of the code. Since the models for heat transfer and flow losses in porous debris in the lower head were designed for general application, a design is also described for implementation of these models into the analysis of porous debris in the core region. An assessment was performed of the capability of the implemented models to calculate the heat transfer and flow losses in porous debris. The assessment showed that SCDAP/RELAP5 is capable of calculating the heat transfer and flow losses occurring in porous debris regions that may develop in a LWR during a severe accident.

CONTENTS

FIGURES

TABLES

1. Introduction

A bed of porous debris may accrete in the lower head of a reactor vessel during a severe accident. If the porous debris is deep and covered with water, then a calculation needs to be made to determine whether the debris bed will locally dry out and heat up in spite of being covered with water. If the debris bed is hot and dry, then the reflood of the debris bed results in a quenching process that needs to be modeled to calculate the transient cooling of the debris bed.

The SCDAP/RELAP5[1] nodalization for analysis of a porous debris bed cooled with water is shown in Figure 1-1. The hydrodynamic phenomenon in the debris bed are calculated by the field equations of RELAP5 and the heatup of the debris is calculated by the COUPLE model in SCDAP/RELAP5. RELAP5 calculates variables such as the velocity and temperature of the fluid in the interstices of the porous debris. The temperatures in the debris and structure wall are determined by the COUPLE model. The RELAP5 model and COUPLE model are connected through the boundary condition of convective heat transfer. Figure 1-2 is a schematic diagram showing the modeling of the debris in the lower head. There are two sets of nodalization that overlap each other, one for the RELAP5 calculation, the other for the COUPLE model. All debris particles within a COUPLE node have the same temperature and all COUPLE nodes within a RELAP5 control volume have the same fluid conditions at the surface of the debris particles represented by that node. A COUPLE node represents all the debris particles from its center to the mid-planes between it and the surrounding nodes.

The COUPLE model in SCDAP/RELAP5 is intended to calculate the heatup of the lower head and the debris that it supports. Previously, the COUPLE model had the capability to model convective and radiative heat transfer from the surfaces of nonporous debris in a detailed manner and to model only in a simplistic manner the heat transfer from porous debris to the fluid in the interstices of the porous debris. If water was present anywhere in porous debris, the entire porous debris bed was assumed to be quenched and all of the debris bed heat generation was transferred to boiling of water, which resulted in a reduction of the amount of water inside the porous debris. After all of the water had boiled off, then the debris bed was assumed to be cooled only at its outer boundaries. In order to advance beyond these simplifications in modeling, designs were developed for a detailed calculation of the heat transfer and flow losses in porous debris. This report describes these designs and their implementation into SCDAP/RELAP5.

This report is organized as follows. Section 2 describes the COUPLE model and Section 3 summarizes the governing equations used in the RELAP5 code. Section 4 describes the interfacing of RELAP5 and COUPLE. This section identifies the variables calculated by COUPLE that are applied by RELAP5 and the variables calculated by RELAP5 that are applied by COUPLE. Section 5 identifies the correlations and models for convective heat transfer that were implemented into the COUPLE model. These correlations have been previously compiled and subjected to peer review.[2,3] Section 6 describes the basic features for implementation of the models for convective heat transfer. Models for flow losses and interphase heat transfer are described in Section 7 and the implementation of these models is described in Section 8. The implementation of the models developed for analysis of porous debris in the lower head resulted in a straightforward application of these models to the analysis of porous debris in the core region. This application is described in Section 9. Section 10 presents results of the assessment of the implemented models. A summary of the extensions in modeling is given in Section 11. The references are listed in Section 12.

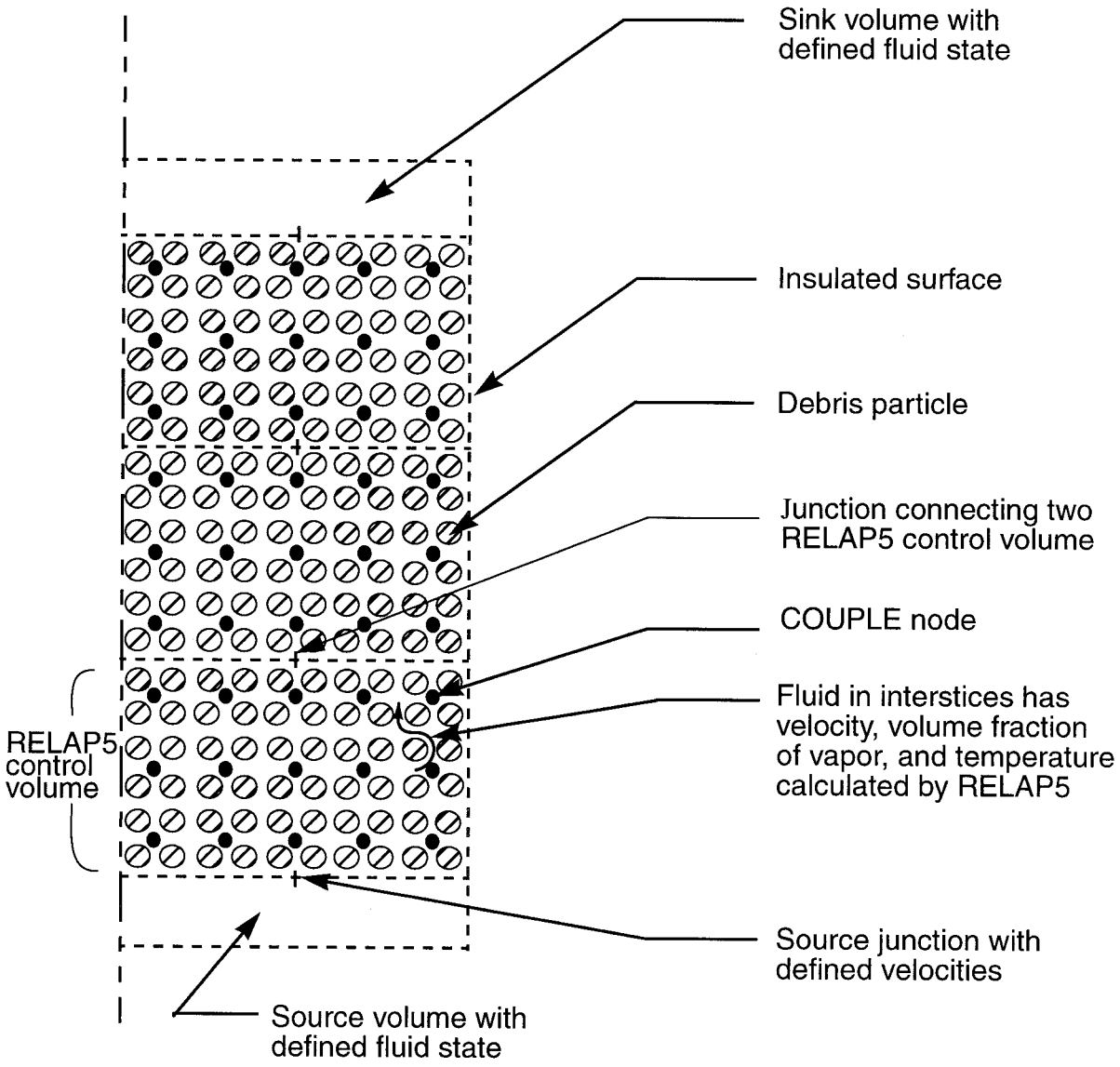

Figure 1-1 Example of RELAP5 and COUPLE nodalization for analysis of porous debris bed cooled by water.

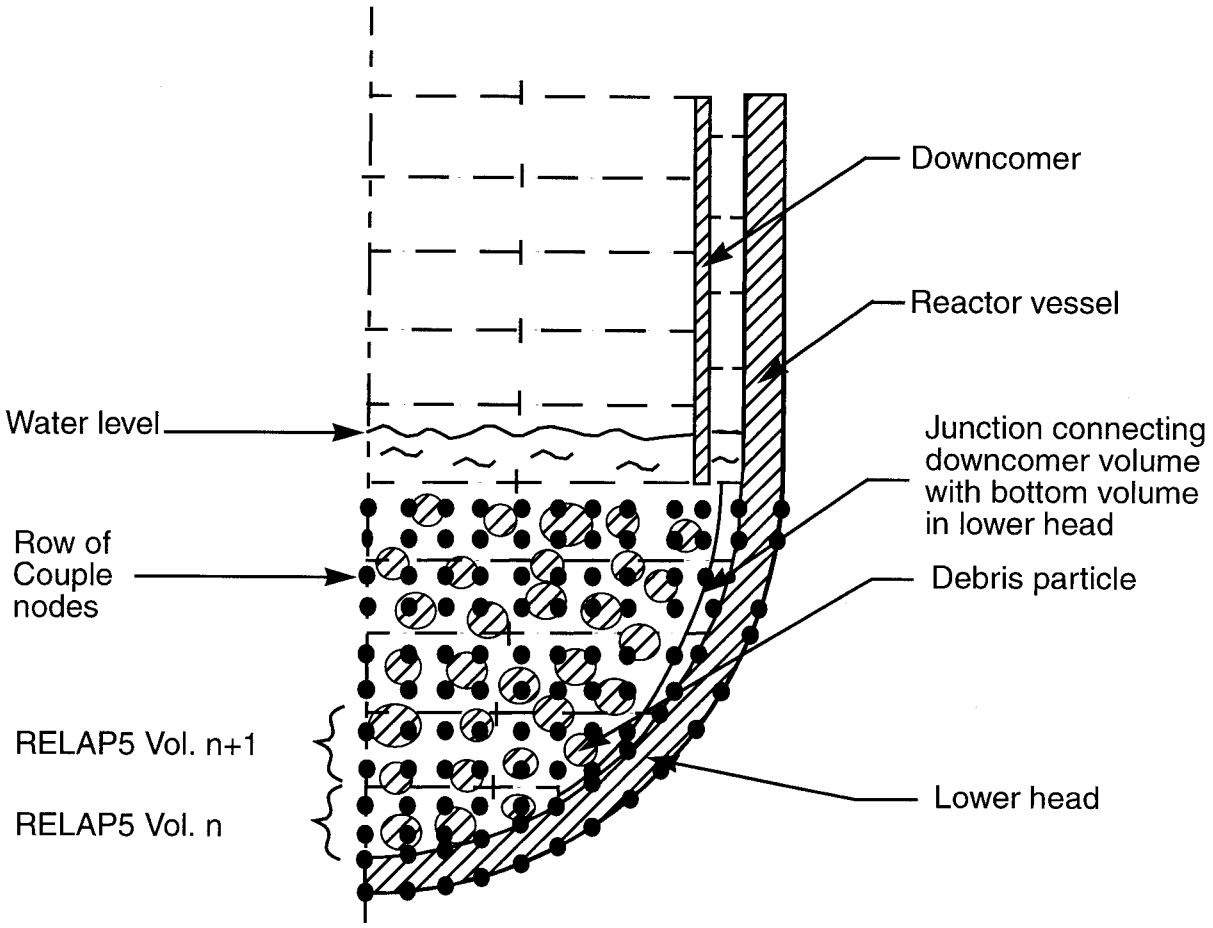

Figure 1-2 Schematic of RELAP5 and COUPLE nodalization of fluid and debris in lower head of reactor vessel.

2. Two-dimensional Debris and Surrounding Structures Model

A model based upon the COUPLE[4] code is used to calculate the heatup of reactor core material that slumps to the lower head of the reactor vessel and is subsequently represented as debris. This model takes into account the decay heat and initial internal energy of slumped debris and then calculates the transport by conduction of this heat in the radial and axial directions to the wall structures and water surrounding the debris. An important use of this model is the calculation of the heatup of the lower head of the reactor vessel in response to contact with material from the core region slumping into it. This calculated heatup is used by models in SCDAP/RELAP5 that evaluate the structural integrity of the lower head. Notable capabilities of the COUPLE model include the modeling of the following phenomena and conditions: (a) spatially varying porosity, (b) thermal conductivity of porous material, (c) a debris bed whose height grows sporadically with time, (d) radiation heat transfer in a porous material, and (e) natural circulation of melted debris. The limitations of this model are: (a) molten material does not flow into an adjacent porous region, (b) oxidation does not occur in the debris bed, and (c) fission product release does not occur in the debris bed.

2.1 COUPLE Description

The COUPLE model performs a two-dimensional, finite element based calculation of steady-state and transient heat conduction. The model was developed to solve both plane and axisymmetric type heat transfer problems with anisotropic thermal properties, subject to boundary conditions of the first kind, second kind, and third kind (combination of the first and second), and/or nonlinear boundary conditions such as radiation. A boundary condition of the first kind implies that the temperatures are prescribed along the boundary surface. A boundary condition of the second kind implies that the normal derivatives of the temperatures are prescribed at the boundary surface. The model solves the following two-dimensional energy equation:

$$(1-\varepsilon)\rho_D c_D \frac{\partial}{\partial t}(T) = \frac{\partial}{\partial x}\left(k_e \frac{\partial T}{\partial x}\right) + \frac{\partial}{\partial y}\left(k_e \frac{\partial T}{\partial y}\right) + Q \qquad (2\text{-}1)$$

where

ρ_D = density of debris particles (kg/m^3),

c_D = heat capacity of debris particles $(J/kg \cdot K)$,

k_e = effective thermal conductivity $(W/m \cdot K)$,

Q = volumetric heat generation rate (W/m^3),

T = temperature of mixture of debris and interstitial fluid (K),

ε = porosity (pore volume/total volume).

The boundary conditions for equation (2-1) are defined by the code user. Boundary conditions are defined for the bottom and top surfaces, and left and right surfaces of the region being represented by the COUPLE model. The boundary conditions at these surfaces can be either adiabatic surface or convection and radiative heat transfer to fluid represented by the RELAP5 code.

2.2 Variable Element Porosity

The COUPLE model allows each element in the debris bed model to have the porosity resulting from the conditions in that element. The porosity of each element can vary with time. The thermal property of each element is determined by

$$\Phi = \varepsilon\phi_f + (1 - \varepsilon)\,\phi_s \tag{2-2}$$

where

Φ = average thermal property value, such as thermal conductivity or specific heat,

ϕ = thermal property,

f = fluid,

s = solid.

If the porosity is zero, the element represents a volume containing solid debris material, whereas a porosity value of 1.0 means the element is completely filled with fluid. A value between 0.0 and 1.0 indicates that the volume contains both fluid and debris material.

2.3 Thermal Conductivity Model

The heat transfer in a dry porous bed involves both conduction and radiation. The overall thermal conductivity of the bed can be represented as

$$k_e = k_{ec} + k_r \tag{2-3}$$

where

k_e = effective conductivity $(W/m \cdot K)$,

k_{ec} = effective conductivity (conduction only) $(W/m \cdot K)$,

k_r = radiative conductivity $(W/m \cdot K)$.

A number of thermal conductivity models have been proposed for modeling a dry porous bed. Reference 5 gives a good review and comparison of five such models. The Imura-Takegoshi[6] model for thermal conductivity combined with the Vortmeyer[7] radiation model yields a good overall result and produces an upper bound on the temperature.

The Imura-Takegoshi model[6] in equation form is given as follows:

$$k_{ec} = \left[\Psi + \frac{1-\Psi}{\phi + \frac{1-\phi}{\nu}}\right] k_g \tag{2-4}$$

$$\phi = 0.3 P \varepsilon^{1.6} \upsilon^{-0.044} \tag{2-5}$$

$$\upsilon = \frac{k_s}{k_g} \tag{2-6}$$

$$\Psi = \frac{\varepsilon - \phi}{1-\phi} \tag{2-7}$$

where

k_g = thermal conductivity of fluid or vapor in pores $(W/m \cdot K)$,

k_s = thermal conductivity of solid material $(W/m \cdot K)$,

ε = porosity of debris.

The Vortmeyer model[7] is given as

$$k_r = 4\eta\sigma d_p T^3 \tag{2-8}$$

where

η = radiation exchange factor (user-defined value, with default value of 0.8),

σ = Stefan-Boltzmann constant $W/m^2 \cdot K^4$ (5.668×10^{-8}),

d_p = particle diameter (m),

T = temperature (K).

The combined Imura-Takegoshi and Vortmeyer model is programmed in the CNDUCT subroutine of COUPLE.

A lower bound model is available in the literature which combines a conduction model by Wilhite[8] with a radiation model by Luikov.[9] This lower bound model has not been applied by the COUPLE model.

2.4 Phase Change Model

At the present time, there are two generally accepted ways of numerically approximating a phase change problem. One method uses a moving mesh technique. At this time, the moving mesh technique has been mainly applied to one-dimensional problems. This technique is not easily applied to two-dimensional problems because mesh distortion may result.

The other method uses a fixed mesh and is usually referred to as an enthalpy method. The particular method that has been chosen is described in Reference 5. The method consists of using the material enthalpy to determine an effective density times specific heat (ρC_p) value to use in Equation (2-1). The enthalpy change per unit volume is defined as

$$dH = \rho C_p dT \tag{2-9}$$

thus,

$$\rho C_p = \frac{dH}{dT} \tag{2-10}$$

which can be written as

$$\rho C_p = \left(\frac{dH}{dX}\right)\left(\frac{dX}{dT}\right) \tag{2-11}$$

where X is the coordinate boundary of a phase change (m).

For computational purposes, it is easier to calculate $\frac{dH}{dX}$ and $\frac{dX}{dT}$ than it is $\frac{dH}{dT}$ directly. The necessary coding required to use this approach is contained in the subroutine USERP.

2.5 Heat Transfer at Surface of COUPLE Finite-Element Mesh

There are two types of boundary conditions that may be applied at the surface of the COUPLE finite element mesh. The first type makes use of a connection to a hydrodynamic volume, thereby allowing heat transfer to and from a surrounding fluid. The second type of boundary condition is applied to the exterior surface of a hemispherical reactor vessel lower head. This boundary condition applies a set of boiling curves to evaluate the heat transfer occurring during reactor vessel cavity flooding.

2.5.1 Hydrodynamic Boundary Condition

Convective and radiative heat transfer boundary conditions may be applied at all external surfaces of a COUPLE model network of nodes (COUPLE mesh). Convective heat transfer coefficients and radiation sink temperatures are determined at the surfaces of the COUPLE model network of nodes through interfaces with the RELAP5 code[10]. The boundary conditions are

$$-k_e(z_b, r_b)\frac{\partial}{\partial n}T(z_b, r_b) = h_c(z_b, r_b)[T(z_b, r_b) - T_c(z_b, r_b)] + q_{rad}(z_b, r_b) \quad (2\text{-}12)$$

where

$T(z_b,r_b)$ = temperature of external surface of node on COUPLE mesh with coordinates of z_b, r_b (K),

$k_e(z_b, r_b)$ = effective thermal conductive at location with coordinates (z_b, r_b) $\left(\frac{W}{m \cdot K}\right)$,

z_b = elevation of node on external surface of mesh (m),

r_b = radius of node on external surface of mesh (m),

n = coordinate in direction normal to external surface (m),

$h_c(z_b,r_b)$ = RELAP5-calculated convective heat transfer coefficient for node on external surface with coordinates z_b,r_b $(W/m^2 \cdot K)$,

$T_c(z_b,r_b)$ = RELAP5 calculated temperature of the fluid at surface coordinates z_b, r_b (K),

$q_{rad}(z_b,r_b)$ = radiation heat flux (W/m^2).

2.5.2 Ex-Vessel Heat Transfer

The USNRC has sponsored an experimental program to evaluate the heat transfer from the outside of a hemispherical reactor vessel which has been flooded. In order to allow the code user to assess the effects of flooding of the reactor vessel cavity, a set of experimental boiling curves has been implemented. The heat transfer data consist of

- A set of correlations describing the heat flux as a function of contact angle and ΔT between the vessel surface and a bulk temperature.
- A correlation for Critical Heat Flux as a function of contact angle.

The set of nucleate boiling curves for heat transfer from the outside of a flooded reactor vessel are of the form: $q'' = a\Delta T + b\Delta T^2 + c\Delta T^3$. Two sets of constants for each of five locations along the hemispherical lower vessel head were determined. One set of constants was for heat transfer to a bulk temperature of 90 ^oC and a second set for heat transfer to a bulk temperature of 100 ^oC (at atmospheric pressure). These constants are defined in Table 2-1.

Table 2-1. Nucleate boiling correlation constants.

l/D[a]	a		b		c	
	90 °C	100 °C	90 °C	100 °C	90 °C	100 °C
0.00		3840	319	334	-2.83	-4.54
0.20	4016	5530	430	380	-4.13	-5.63
0.35		515	337	1109	2.61	-18.50
0.50			891	960	-9.04	-8.18
0.75			529	134	0.08	13.00

a. l/D is the ratio of the distance from the centerline of the vessel to the radius of the hemispherical head. The angle of contact is $0.5\pi\left(\frac{l}{d}\right)$.

These correlations yield a boiling curve as a function of the temperature difference between vessel surface and a bulk temperature, with a valid range from approximately 4 °K to the temperature difference which causes a critical heat flux (CHF). The correlation for CHF as a function of contact angle is

$$q_{chf} = 0.4(1 + 0.021\theta - (0.007\theta)^2)(1 + 0.036\Delta T_{sub}) \quad (2\text{-}13)$$

where

q_{chf} = the critical heat flux in MW/m^2,

θ = the contact angle,

Δt_{sub} = the degree of subcooling.

This experimental data was applied in the following manner:

Nucleate Boiling:

- For a ΔT (between vessel surface and bulk temperature) between 0 and 4 K, a linear interpolation is applied between a heat flux of zero at zero ΔT to the heat flux predicted by the appropriate correlation at a ΔT of 4 K.

- Between a ΔT of 4 K and the ΔT which corresponds to CHF, the appropriate correlation is used. The ΔT at CHF is determined by iteratively increasing the ΔT until either the predicted critical heat flux is reached or the heat flux predicted by the correlation begins to decrease.

Transition:

- After Critical Heat Flux is reached, the predicted transition heat flux is linearly extrapolated from the CHF to a user-defined heat transfer coefficient to vapor.

Vapor Heat Transfer:

- Heat transfer to vapor is modeled when a location on the external surface of the lower head is uncovered. This rate of heat transfer is governed by a user-defined heat transfer coefficient. The heat flux is not permitted to decrease below the heat flux predicted with this user-defined value.

An application of the data for saturated conditions is shown graphically in Figure Figure-2-1 for each of the specified contact angles.

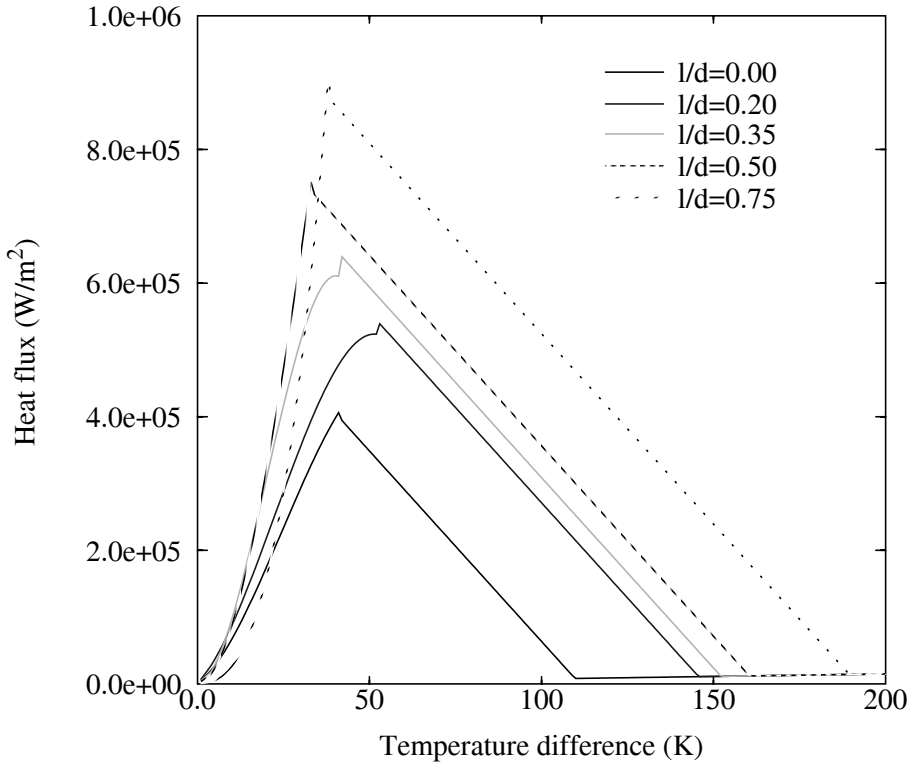

Figure 2-1 Predicted heat flux from ex-vessel heat transfer correlations as a function of position and temperature.

2.6 Heat Transfer at Interface of Debris Region and Structure

The rate of heat transfer from a debris region into a structure in contact with the debris is a strong function of the conditions at the interface between the debris and structure. The modeling of this heat transfer is performed using the concept of a null element, which is an element with zero volume and whose nodes overlay the interface between the debris and the structure. Null elements are defined by the code user along possible interfaces between debris and structure. The heat transfer through the null elements is calculated by the equation

$$q_i = h_{gap} (T_d - T_s) \qquad (2\text{-}14)$$

where

q_i = heat flux across the interface,

h_{gap} = heat transfer coefficient for interface between debris and structure $(W/m^2 \cdot K)$. (This variable is defined by the code user and the suggested default value is 500 $W/m^2 \cdot K$),

T_d = temperature of debris at the interface (K),

T_s = temperature of structure at the interface (K).

The debris and structure nodes have the same coordinates but different identification numbers. The debris node is part of a finite element modeling the debris and the structure node is part of a finite element modeling the structure in contact with the debris. The heat flux calculated by Equation (2-14) is applied at both the surface of the finite element with debris that faces the structural element and the surface of the structural element that faces the debris element.

The modeling of the gap heat transfer coefficient is divided into three regimes: (1) solidified debris, (2) partially liquefied debris, and (3) completely liquefied debris. For the solidified debris regime, the heat transfer is a function of the surface roughness of the debris and structure and of other parameters. For this regime, the debris model does not attempt to calculate the gap heat transfer coefficient. Instead, the gap heat transfer coefficient is defined from user input. In the liquefied debris regime, the gap heat transfer coefficient is set to a value of 10,000 W/m^2•K, which in effect defines the thermal resistance at the gap to be zero. In the partially liquefied regime, the heat transfer coefficient is calculated by the equation

$$h_{gap} = h_{liq} + (h_{us} - h_{liq})(T_{liq} - T_{DI})/(T_{liq} - T_{sol}) \quad (2\text{-}15)$$

where

h_{liq} = heat transfer coefficient for interface for case of debris at interface being completely liquefied (10,000 $W/m^2 \cdot K$),

h_{us} = user-defined heat transfer coefficient for interface between debris and structure $(W/m^2 \cdot K)$,

T_{liq} = liquidus temperature of debris at interface (K),

T_{DI} = temperature of debris at interface with structural material (K),

T_{sol} = solidus temperature of debris at interface (K).

The value of (T_{liq} - T_{sol}) is assumed to be 43 K, which is appropriate for a mixture of UO_2 and ZrO_2.

3. RELAP5 Hydrodynamic Model

The RELAP5[11] thermal-hydraulic model solves eight field equations for eight primary dependent variables. The primary dependent variables are pressure (P), phasic specific internal energies (U_g, U_f), vapor volume fraction (void fraction) (α_g), phasic velocities (v_g, v_f), noncondensable quality (X_n), and boron density (ρ_b). The independent variables are time (t) and distance (x). A detailed description on the formulation of field equations is given in Reference 11. The differential form of conservation of mass, momentum and energy equations is first presented to facilitate the description of how RELAP5 will be used to model flow in a porous debris medium. A discussion of the finite difference equations will then follow.

Mass Conservation

The phasic continuity equations are

$$\frac{\partial}{\partial t}(\alpha_g \rho_g) + \frac{1}{A}\frac{\partial}{\partial x}(\alpha_g \rho_g v_g A) = \Gamma_g \tag{3-1}$$

$$\frac{\partial}{\partial t}(\alpha_f \rho_f) + \frac{1}{A}\frac{\partial}{\partial x}(\alpha_f \rho_f v_f A) = -\Gamma_g \tag{3-2}$$

where

A = cross-section area (m^2),

α_g = vapor volume fraction (void fraction),

α_f = liquid volume fraction, $\alpha_f = 1 - \alpha_g$,

ρ_g = vapor density (k_g/m^3),

ρ_f = liquid density (k_g/m^3),

v_g = vapor velocity (m/s),

v_f = liquid velocity (m/s),

Γ_g = total volumetric mass transfer rate $(k_g/m^3 \cdot s)$.

The interfacial mass transfer model assumes that total mass transfer can be partitioned into mass transfer at the vapor/liquid interface in the bulk fluid and mass transfer at the vapor/liquid interface in the boundary layer near the walls; that is,

$$\Gamma_g = \Gamma_{ig} + \Gamma_w \ . \tag{3-3}$$

where

Γ_{ig} = volumetric mass transfer rate at the vapor/liquid interface in the bulk fluid $(k_g/m^3 \cdot s)$,

Γ_w = volumetric mass transfer rate at the vapor/liquid interface in the boundary layer near the wall $(k_g/m^3 \cdot s)$.

Momentum Conservation

The phasic conservation of momentum equations are used, and recorded here, in an expanded form and in terms of momenta per unit volume using the phasic primitive velocity variables v_g and v_f. The spatial variation of momentum term is expressed in terms of v_g^2 and v_f^2. The momentum equation for the vapor phase is

$$\begin{aligned}\alpha_g\rho_g A\frac{\partial v_g}{\partial t}+\frac{1}{2}\alpha_g\rho_g A\frac{\partial v_g^2}{\partial x} &= -\alpha_g A\frac{\partial P}{\partial x}+\alpha_g\rho_g B_x A-(\alpha_g\rho_g A)FWG(v_g)+\alpha_g\rho_g H_{lossg}\frac{(\partial v)}{\partial x}A\\ &+\Gamma_g A(v_I-v_g)-(\alpha_g\rho_g\alpha_f\rho_f A)FI(v_g-v_f)\\ &-C\alpha_g\alpha_f\rho_m A\left[\frac{\partial(v_g-v_f)}{\partial t}+v_f\frac{\partial v_g}{\partial x}-v_g\frac{\partial v_f}{\partial x}\right]\end{aligned} \tag{3-4}$$

and for the liquid phase is

$$\begin{aligned}\alpha_f\rho_f A\frac{\partial v_f}{\partial t}+\frac{1}{2}\alpha_f\rho_f A\frac{\partial v_f^2}{\partial x} &= -\alpha_f A\frac{\partial P}{\partial x}+\alpha_f\rho_f B_x A-(\alpha_f\rho_f A)FWF(v_f)\\ &-\Gamma_g A(v_I-v_f)-(\alpha_g\rho_g\alpha_f\rho_f A)FI(v_f-v_g)\\ &-C\alpha_f\alpha_g\rho_m A\left[\frac{\partial(v_f-v_g)}{\partial t}+v_g\frac{\partial v_f}{\partial x}-v_f\frac{\partial v_g}{\partial x}\right].\end{aligned} \tag{3-5}$$

where

B_x = body force (m/s^2),

C = coefficient of virtual mass,

FWG = vapor wall drag coefficients (s^{-1}),

FWF = liquid wall drag coefficients (s^{-1}),

FI = interphase drag coefficient $(m^3/kg \cdot s)$,

P = pressure (Pa),

v_I = velocity at interface between vapor and liquid (m/s).

The force terms on the right sides of Equations (3-4) and (3-5) are, respectively, the pressure gradient, the body force (i.e., gravity and pump head), wall friction, momentum transfer due to interface mass transfer, interface frictional drag, and force due to virtual mass. The terms FWG and FWF are part of the wall frictional drag, which are linear in velocity, and are products of the friction coefficient, the frictional reference area per unit volume, and the magnitude of the fluid bulk velocity. The interfacial velocity in the interface momentum transfer term is the unit momentum with which phase appearance or disappearance occurs. The coefficient FI is part of the interface frictional drag; two different models (drift flux and drag coefficient) are used for the interface friction drag, depending on the flow regime. The coefficient of virtual mass C is calculated according to the flow regime.

Energy Conservation

The phasic thermal energy equations are

$$\frac{\partial}{\partial t}(\alpha_g \rho_g U_g) + \frac{1}{A}\frac{\partial}{\partial x}(\alpha_g \rho_g U_g v_g A) = -P\frac{\partial \alpha_g}{\partial t} - \frac{P}{A}\frac{\partial}{\partial x}(\alpha_g v_g A) + Q_{wg} + Q_{ig} + \Gamma_{ig} h_g^* + \Gamma_w h_g' + DISS_g \tag{3-6}$$

$$\frac{\partial}{\partial t}(\alpha_f \rho_f U_f) + \frac{1}{A}\frac{\partial}{\partial x}(\alpha_f \rho_f U_f v_f A) = -P\frac{\partial \alpha_f}{\partial t} - \frac{P}{A}\frac{\partial}{\partial x}(\alpha_f v_f A) + Q_{wf} + Q_{if} - \Gamma_{ig} h_f^* - \Gamma_w h_f' + DISS_f \ . \tag{3-7}$$

where

h_f^* = liquid enthalpy associated with interface mass transfer in the bulk (J/kg),

h_g^* = vapor enthalpy associated with interface mass transfer in the bulk (J/kg),

h_f' = liquid enthalpy associated with interface mass transfer near the wall (J/kg),

h_g' = vapor enthalpy associated with interface mass transfer near the wall (J/kg),

Q_{wf} = wall heat transfer rate per unit volume to liquid (W/m^3),

Q_{wg} = wall heat transfer rate per unit volume to vapor (W/m^3),

U_f = liquid specific internal energy (J/kg),

U_g = vapor specific internal energy (J/kg).

In the phasic energy equations, Q_{wg} and Q_{wf} are the phasic wall heat transfer rates per unit volume. These phasic wall heat transfer rates satisfy the equation

$$Q = Q_{wg} + Q_{wf} \tag{3-8}$$

where Q is the total wall heat transfer rate to the fluid per unit volume.

The phasic enthalpies (h_g^*, h_f^*) associated with bulk interface mass transfer in Equations (3-6) and (3-7) are defined in such a way that the interface energy jump conditions at the liquid-vapor interface are satisfied. In particular, the h_g^* and h_f^* are chosen to be h_g^s and h_f, respectively, for the case of vaporization and h_g and h_f^s, respectively, for the case of condensation. The same is true for the phasic enthalpies (h_g', h_f') associated with wall (thermal boundary layer) interface mass transfer. The logic for this choice depends on the mass transfer (vapor generation) model. In particular, it can be shown that h_g^* and h_f^* should be

$$h_g^* = \frac{1}{2}[(h_g^s + h_g) + \eta(h_g^s - h_g)] \tag{3-9}$$

and

$$h_f^* = \frac{1}{2}[(h_f^s + h_f) - (h_f^s - h_f)] \tag{3-10}$$

where

η = 1 for $\Gamma_{ig} \geq 0$,

= -1 for $\Gamma_{ig} < 0$,

h_f = liquid specific enthalpy (J/kg),

h_g = vapor specific enthalpy (J/kg),

h_f^s = saturation liquid specific enthalpy (J/kg),

h_g^s = saturation vapor specific enthalpy (J/kg).

It can also be shown that h_g' and h_f' should be

$$h_g' = \frac{1}{2}[(h_g^s + h_g) + \lambda(h_g^s - h_g)] \tag{3-11}$$

and

$$h_f' = \frac{1}{2}[(h_f^s + h_f) - (h_f^s - h_f)] \tag{3-12}$$

where

λ = 1 for $\Gamma_w \geq 0$,

= -1 for $\Gamma_w < 0$.

The numerical solution scheme is based on replacing the differential equations with finite difference equations partially implicit in time. The difference equations are based on the concept of control volumes and a staggered spatial mesh. The pressures, energies, and void fractions are defined at volumes, and velocities are defined at junctions. When the momentum equations are finite differenced (using integration over the momentum control volume which is centered on a junction), additional terms on the right side appear at the junction and are of the form

$$-\alpha_g \rho_g HLOSSGv_g - \alpha_f \rho_f HLOSSGv_f \tag{3-13}$$

for the sum momentum equation and of the form

$$-HLOSSGv_g + HLOSSGv_f \tag{3-14}$$

for the difference momentum equation. The HLOSSG and HLOSSF terms contain both code calculated abrupt area change loss terms and user-specified loss terms. This is discussed further in Reference 11.

4. Interface of RELAP5 and COUPLE and Assumptions in Modeling

The RELAP5 code and COUPLE model interact with each other at each time step. RELAP5 provides COUPLE with the hydrodynamic conditions within the interstices of the debris particles. These conditions include: (1) velocities of liquid and vapor phases, (2) temperatures of liquid and vapor phases, (3) pressure, and (4) volume fractions of liquid and vapor. The COUPLE model calculates the heat transfer from the debris to the fluid in the hydrodynamic volumes containing debris. The subroutine in RELAP5 named HLOSS calculates the HLOSSF, HLOSSG and FI terms at locations with porous debris to represent the flow losses and interphase drag in a porous debris medium.

The following assumptions are applied to simplify the calculation of heat transfer and flow losses in porous debris:

1. Radiation heat transfer is not be modeled at locations with two-phase coolant.

2. Conductive heat transfer in debris is neglected at locations where liquid water is present; at these locations heat transfer by convection dominates over heat transfer by conduction. This assumption is applied by setting effective thermal conductivities to zero at locations where liquid water is present.

3. Debris particles are assumed to be spherical, uniform in size, and with regular packing. Since the code does not have a model to generate a mixture of particles of nonuniform size or non-spherical shape, this assumption is not restrictive.

4. Debris particles are greater than the smallest possible bubble size, which is assumed to be 3.5 mm.

5. Porosity is assumed to range between 0.4 and 0.5. This assumption keeps the debris porosity within the range of application of most of the correlations applied to calculate heat transfer and flow losses.

6. The boundaries between flow regimes are as defined by Tung.[12] While the physical basis for these boundaries is not well-established, the presentation of a more thorough physical basis is beyond the scope of this work. The void fraction at which the flow regime changes from inverted slug-mist flow to mist flow is assumed to be 0.925.

7. The mesh size for the COUPLE model is significantly larger than the size of the debris particles. The satisfaction of this requirement maintains the applicability of the convective heat transfer models for porous debris.

The exchange of information between various models in RELAP5 and COUPLE is shown in Figure Figure-4-1 This exchange in information results in RELAP5 calculating the flow losses and the state of the fluid in the interstices of the porous debris and COUPLE calculating the convective heat transfer from debris using the RELAP5 calculated state of the fluid.

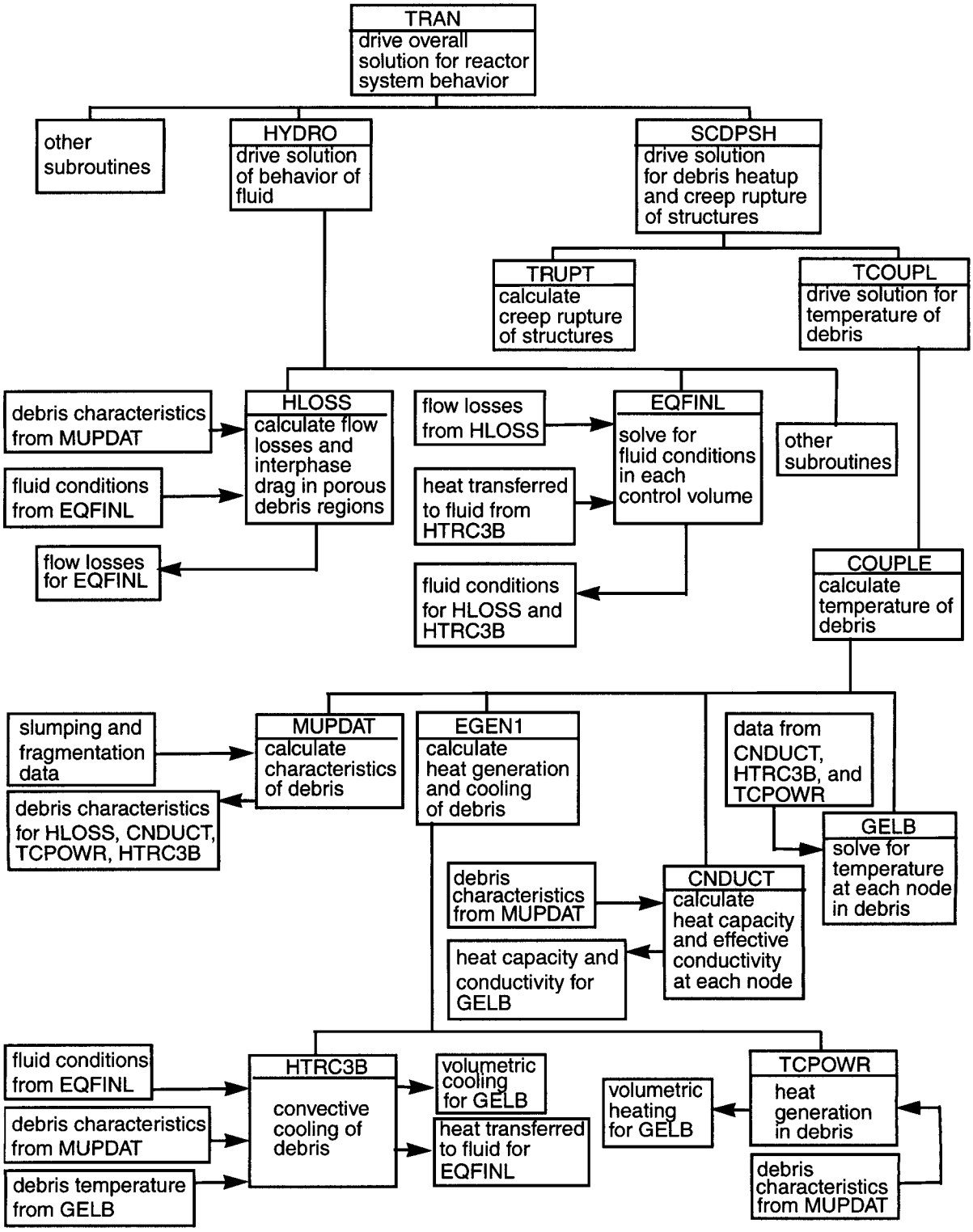

Figure 4-1 Flow chart of information exchanged between various SCDAP/RELAP5 subroutines in order to calculate heatup of porous debris.

5. Review of Models for Heat Transfer between Porous Debris and Interstitial Fluid

This section reviews models for convective and radiative heat transfer that have been previously published and subjected to peer review[2,3], and which have been incorporated into the COUPLE model. Six regimes of convective heat transfer are identified and correlations for heat transfer are obtained for each regime. Equations are also presented for calculating the radiative heat transfer between porous debris and the interstitial fluid.

The regimes of convective heat transfer are distinguished by the values of two parameters; (1) volume fraction of liquid in the open porosity of the coolant, and (2) temperature of the debris. The regimes of heat transfer range from nucleate boiling in two-phase coolant to natural convection in steam. The various regimes of convective heat transfer and the corresponding ranges in values of volume fraction of liquid and debris temperature are identified in Table 5-1. The symbols used in Table 5-1 are defined in Table 5-2. In Table 5-1 several temperature thresholds are identified for transition from one regime of heat transfer to another regime of heat transfer. One of these temperature thresholds, namely T_{sat}, is determined by the water properties package for SCDAP/RELAP5. Another threshold temperature, namely T_{TF}, is determined from experimental results. The other temperature thresholds are determined by matching a heat flux from one regime of heat transfer with the heat flux from the adjacent regime of heat transfer.

Table 5-1. Regimes of convective heat transfer and corresponding ranges in values of volume fraction of liquid and debris temperature.

Phase state of fluid	Mode of heat transfer	Range of void fraction of vapor	Range of debris temperature (K)
single phase vapor	*forced convection and natural convection*	*1.0*	$T_D > T_{sat}$
single phase liquid	*forced convection and natural convection*	*0.0*	$T_D \leq T_{sat}$
two-phase	*nucleate boiling*	$0.0 \leq \alpha_g < \alpha_4$	$T_{CN} < T_D < T_{nuc}$
two-phase	*transition boiling*	$0.0 \leq \alpha_g < \alpha_4$	$T_{nuc} < T_D < T_{TF}$
two-phase	*film boiling*	$\alpha_g \leq \alpha_4$	$T_D > T_{TF}$
two-phase	*transition from film boiling to convection to vapor*	$\alpha_4 \leq \alpha_g < 1.0$	$T_D > T_{TF}$

Table 5-2. Definition of symbols in Table 5-1.

Symbol	Units	Definition
α_g	- -	*volume fraction of vapor in fluid*
T_D	*K*	*temperature of debris*
T_{sat}	*K*	*saturation temperature of fluid*

Table 5-2. Definition of symbols in Table 5-1. (continued)

Symbol	Units	Definition
T_{CN}	K	*temperature of debris at which heat flux using convection correlation equals heat flux using nucleate boiling correlation*
T_{nuc}	$-K$	*temperature of debris at which heat flux using nucleate boiling correlation equals critical heat flux*
T_{TF}	K	*temperature of debris at which transition boiling heat transfer ends and film boiling heat transfer begins*
α_4	- -	*void fraction at which flow regime changes from inverted slug-mist flow to mist flow (~0.925).*

5.1 Single Phase Vapor Regime

The heat transfer correlation developed by Tung[12] is used to calculate the debris-to-vapor convective heat transfer. In this correlation, the Nusselt number is given by the equation

$$Nu_{conv} = 0.27 Re^{0.8} Pr^{0.4} \tag{5-1}$$

where

Nu_{conv} = Nusselt number for convection,

Re = Reynold's number,

Pr = Prandtl number.

The Nusselt number for convection is given by the equation

$$Nu_{conv} = (hD_p)/k_g \tag{5-2}$$

where

h = convective heat transfer coefficient $(W/m^2 \cdot K)$,

D_p = effective diameter of debris particle (m),

k_g = thermal conductivity of vapor $(W/m \cdot K)$.

The Reynold's number is given by the equation

$$Re = \rho_g v_g D_p / \mu_g \tag{5-3}$$

where

ρ_g = density of vapor (kg/m^3),

v_g = velocity of vapor (m/s),

D_p = effective diameter of debris particle (m),

μ_g = viscosity of vapor $(kg/m \cdot s)$.

The Prandtl number is given by the equation

$$Pr = \mu_g c_g / k_g \tag{5-4}$$

where

μ_g = viscosity of vapor $(kg/m \cdot s)$,

c_g = heat capacity of vapor $(J/kg \cdot K)$,

k_g = thermal conductivity of vapor $(W/m \cdot K)$.

The ranges of parameters for which this correlation is based are

$$0.7 \le Pr \le 5$$

$$18 \le Re \le 2400$$

$$0.4 \le \varepsilon \le 0.5 \ .$$

For the case of low fluid velocity, the Nusselt number for natural convection is calculated. If the Nusselt number for natural convection is greater than that for forced convection, then the natural convection Nusselt number is applied. The natural convection Nusselt number is taken from Edwards, Denny and Mills[13] as

$$Nu_{nat} = KRa^{0.25} \tag{5-5}$$

where

Nu_{nat} = Nusselt number for natural convection,

$$K = \begin{cases} 0.3 & 0 \le Ra \le 50 \\ 0.4 & 50 \le Ra \le 200 \\ 0.5 & 200 \le Ra \le 10^6 \\ 0.6 & 10^6 \le Ra \le 10^8 \end{cases}$$

Ra = Rayleigh number.

It should be mentioned that equation (5-5) was originally developed for a single sphere. The underlying hypothesis for applying this correlation to the current porous medium environment is documented in Reference 12.

The Rayleigh number is calculated by the equation

$$Ra = Gr \bullet Pr = \frac{\rho_g^2 g D_p^3 \beta \Delta T}{\mu_g^2} Pr. \quad (5\text{-}6)$$

where

g = acceleration of gravity (m/s^2),

β = volume coefficient of expansion of vapor (1/K),

ΔT = local temperature difference between debris and vapor ($T_D - T_g$).

The heat transferred to the vapor by convection is calculated by the equation

$$Q_{conv} = A_s max(Nu_{conv}, Nu_{nat}) \frac{k_g}{D_p} (T_D - T_g) \quad (5\text{-}7)$$

where

Q_{conv} = heat transferred to vapor by convection (W/m^3),

A_s = surface area of debris per unit volume (m^2/m^3),

T_D = temperature of debris particles (K),

T_g = temperature of vapor (K).

If the value of Re is less than the range of applicability for Nu_{conv} $(Re < 8)$, then only Nu_{nat} is used in Equation (5-7).

The surface area of debris per unit volume is calculated by applying the assumption that the particles are spherical in shape and uniform in size. The resulting equation is

$$A_s = \frac{6(1-\varepsilon)}{D_p} \quad (5\text{-}8)$$

where

ε = porosity of debris.

The heat transferred to the vapor by radiation is calculated by the equation[14]

$$Q_{rad} = A_s F_g \sigma (T_D^4 - T_g^4), \tag{5-9}$$

where

Q_{rad} = heat transferred to vapor by radiation (W/m3),

F_g = gray-body factor,

σ = Stefan-Boltzmann constant (5.668×10^{-8} W/m^{2}K^4).

The gray body factor is calculated by the equation

$$F_g = 1/[R_1(1 + R_3/R_1 + R_3/R_2)] \tag{5-10}$$

where

R_1 = $(1-\varepsilon_g)/\varepsilon_g$,

R_2 = $1/\varepsilon_g$,

R_3 = $1 + (1-\varepsilon_D)/\varepsilon_D$,

ε_g = $1-\exp(-a_g L_m)$,

ε_D = emissivity of debris particles,

a_g = absorption coefficient for vapor,

L_m = mean path length (m).

The absorption coefficient, a_g is calculated by the SCDAP subroutine EMISSV.[1] An estimation of the mean path is obtained by assuming it equal to the hydraulic diameter.[14] Assuming the particles are spheres of uniform size in a regular packed matrix, the hydraulic diameter is estimated by the equation

$$L_m = \frac{4\varepsilon D_p}{6(1-\varepsilon)} \tag{5-11}$$

The total heat transfer to the vapor is then

$$Q = Q_{conv} + Q_{rad} \tag{5-12}$$

where

Q = total heat transfer to vapor (W/m^3).

5.2 Single Phase Liquid Regime

The heat transfer correlation presented by Gunn[15] is used to calculate the volumetric heat transfer coefficient for the covered regime. This correlation is applicable for water that is either subcooled or saturated. The correlation for the Nusselt number is given by the equation

$$Nu = (7 - 10\varepsilon + 5\varepsilon^2)(1 + 0.7Re^{0.3}Pr^{0.333}) + (1.33 - 2.4\varepsilon + 1.2\varepsilon^2)Re^{0.7}Pr^{0.333} \tag{5-13}$$

where

Pr = Prandtl number.

The Prandtl number is calculated by the equation

$$Pr = \mu_f c_f / k_f \tag{5-14}$$

where

μ_f = viscosity of the liquid $(kg/m \cdot s)$,

c_f = heat capacity of the liquid $(J/kg \cdot K)$,

k_f = thermal conductivity of the water $(W/m \cdot K)$.

The Reynold's number is calculated by the equation

$$Re = v_f \rho_f l / \mu_f \tag{5-15}$$

where

v_f = velocity of the liquid (m/s),

ρ_f = density of the liquid (kg/m3),

l = characteristic length as defined below (m).

The volumetric heat transfer coefficient is calculated by the equation

$$h_v = Nu\frac{k_f}{l^2}. \tag{5-16}$$

The characteristic length is calculated by the equation

$$l = b/a \tag{5-17}$$

where

b = inertial coefficient in Kozeny-Carman equation (1/m),

a = viscous coefficient in Kozeny-Carman equation ($1/m^2$).

The coefficients b and a are calculated by the equations

$$b = 1.75(1-\varepsilon)/\varepsilon^3 D_p, \tag{5-18}$$

$$a = 150(1-\varepsilon)^2/\varepsilon^3 D_p^2$$

where

ε = porosity of debris,

D_p = effective diameter of debris particles (m).

The total heat transfer to the fluid is calculated by the equation

$$Q = h_v(T_D - T_f) \tag{5-19}$$

where

Q = total heat transfer to the fluid (W/m^3),

T_D = surface temperature of debris (K),

T_f = temperature of liquid (K).

The heat transfer to the vapor phase and the volumetric vapor generation rate are equal to zero for this heat transfer regime.

The forced convection and natural convection heat transfer to the liquid phase can also be calculated by Equations (5-1) and (5-6) with the properties of the liquid phase substituted in place of properties of the vapor phase.[3] The characteristic length scale can be defined in two different ways for these modes of heat transfer, as is shown by Equations (5-2) and (5-3).[3]

5.3 Debris Heat Transfer for Two-Phase Flow

The debris-to-fluid heat transfer in the two-phase region is a complex process. The heat transfer modeling is made to be consistent with the flow regime modeling. In view of the fact that there is an absence of available experimental data and theoretical models for local heat transfer coefficients for two-phase conditions, a simplified approach is required.

Four modes of convective heat transfer are considered: (1) nucleate boiling; (2) film boiling; (3) transition boiling; and (4) transition from film boiling to convection to vapor. The mode of heat transfer that is in effect is a function of the debris temperature and the volume fraction of vapor in the fluid. The range of conditions for each mode of heat transfer have been summarized in Table 5-1. The symbols in Table 5-1 have been defined in Table 5-2.

5.3.1 Nucleate Boiling

The heat transfer coefficient for nucleate boiling is calculated by a correlation for pool boiling that was developed by Rohsenow[16] and used by Tutu, et al.[24] This correlation is

$$h_{snuc} = 4.63x10^{6} f(prop)(T_D - T_{sat})^{m} \tag{5-20}$$

where

h_{snuc} = heat transfer coefficient for nucleate boiling mode of heat transfer ($W/m^2 \cdot K$),

f(prop) = function that is combination of fluid properties as defined below,

m = exponent that is function of particle diameter as shown below.

The function of fluid properties is

$$f(prop) = \frac{\mu_f c_{pf}^3}{(h_{fg}^2)\left[\frac{\sigma}{g(\rho_f - \rho_g)}\right]^{0.5}\left(\frac{c_{pf}\mu_f}{k_f}\right)^{4.913}} \tag{5-21}$$

where

μ_f = viscosity of liquid water $(kg/m \cdot s)$,

c_{pf} = heat capacity of liquid water $(J/kg \cdot K)$,

h_{fg} = latent heat of vaporization $(J/kg \cdot K)$,

σ = surface tension (kg/s^2),

g = acceleration of gravity (9.8 m/s^2),

ρ_f = density of saturated liquid (kg/m^3),

ρ_g = density of saturated liquid (kg/m^3),

k_f = thermal conductivity of liquid water (W/m·K).

The exponent m is calculated by the equation[3]

$$m = 3.3 - 9.0e^{-d} \tag{5-22}$$

where

$$d = \left\{ \frac{D_p}{\left[\frac{\sigma}{g(\rho_f - \rho_g)}\right]^{0.5}} \right\}^{0.5}.$$

If d is calculated to be less than 1.4142, then d is set to a value of 1.4142 $(m \geq 1.1)$.

The debris temperature at which the transition from the forced convection to single phase liquid mode of heat transfer to the nucleate boiling mode of heat transfer takes place is equal to T_{CN}, which is determined by solving the following equation for T_{CN}:

$$h_v(T_{CN}-T_{sat}) = 4.63\times10^6 f(prop)(T_{CN}-T_{sat})^{m+1} A_s \tag{5-23}$$

where

h_v = volumetric heat transfer coefficient for forced convection to liquid,

T_{CN} = temperature of debris at which heat flux using forced convection correlation equals heat flux using nucleate boiling correlation (K),

A_s = surface area of particles as defined by Equation (5-8) (m^2/m^3).

The maximum temperature of debris for the nucleate boiling mode of heat transfer is determined by solving the following equation for T_{nuc}:

$$4.63\times10^{6} f(prop)(T_{nuc}-T_{sat})^{m}(T_{nuc}-T_{sat}) = q_{CHF} \quad (5\text{-}24)$$

where

T_{nuc} = maximum particle temperature for nucleate boiling mode of heat transfer (K),

q_{CHF} = critical heat flux calculated as shown below (W/m^2).

The critical heat flux is calculated by a correlation for spheres developed by Ded and Lienhard:[17]

$$q_{CHF} = 0.11 F_d h_{fg} \rho_g [g\sigma((\rho_f - \rho_g)/\rho_g^2)]^{0.25} \quad (5\text{-}25)$$

where

F_d = factor correcting for debris particle size as defined below,

h_{fg} = latent heat of vaporization (J/kg),

g = acceleration of gravity (9.8 m/s^2),

ρ_f = density of saturated liquid (kg/m^3),

ρ_g = density of saturated liquid (kg/m^3),

σ = surface tension (kg/s^2).

The factor F_d is calculated by the equation[10]

$$F_d = 1 - 3.8e^{-d} \quad (5\text{-}26)$$

where

$$d = \left\{ \frac{D_p}{\left[\frac{\sigma}{g\rho_f - \rho_g}\right]^{0.5}} \right\}^{0.5}.$$

If d is calculated to be less than 1.4142, then d is set to a value of 1.4142.

5.3.2 Film Boiling

The correlation developed by Dhir and Purohit[18] is used to calculate the surface heat transfer coefficient for the film boiling mode of heat transfer. According to their correlation, the Nusselt number is calculated by the equation

$$Nu = \frac{hD_p}{k_g} = \overline{Nu_0} + \overline{Nu_{nc}}\frac{Pr_g Sc}{Pr_f Sh \mu_f} + \frac{Pr_g}{Sh}\frac{\sigma(T_w^4 - T_{sat}^4)D_p}{h_{fg}\mu_g} \tag{5-27}$$

$$\overline{Nu_0} = 0.8\left[\frac{g\rho_g(\rho_f - \rho_g)h_{fg}D_p^3}{\mu_g k_g \Delta T_w}\right]^{1/4} \tag{5-28}$$

and

$$\overline{Nu_{nc}} = 0.9\left[\frac{g\rho_f^2 - C_{pf}\beta\Delta T_{sub}D_p^3}{\mu_f k_f}\right]^{1/4} \tag{5-29}$$

where

Nu	=	Nusselt number for film boiling mode of heat transfer, hD_p/k_g,
$\overline{Nu_0}$	=	Nusselt number based on the saturated film boiling heat transfer coefficient averaged over the particle, $\bar{h}_0 D_p/k_g$,
$\overline{Nu_{nc}}$	=	Nusselt number based on the natural convection heat transfer coefficient averaged over the particle, $\bar{h}_{nc} D_p/k_f$,
C_{pf}	=	specific heat of liquid $(J/kg \cdot K)$,
D_p	=	effective diameter of particles (m),
g	=	acceleration of gravity (9.8 m/s^2),
h	=	heat transfer coefficient $(K/m^2 \cdot K)$,
$\bar{h}_0$	=	saturated pool film boiling heat transfer coefficient $(K/m^2 \cdot K)$,
$\bar{h}_{nc}$	=	natural convection heat transfer coefficient averaged over the surface of the sphere $(K/m^2 \cdot K)$,
h_{fg}	=	latent heat of vaporization (J/kg),
k_g k_f	=	thermal conductivity of vapor, liquid $(W/m \cdot K)$,

Pr = Prandtl number,

Sc = liquid subcooling parameter, $C_{pf}\Delta T_{sub}/h_{fg}$,

Sh = vapor superheat parameter, $C_{pg}\Delta T_w/h_{fg}$,

T_g = temperature of the vapor (K),

T_{sat} = saturation temperature (K),

T_w = particle surface temperature (K),

ΔT_{sub} = difference between the saturation temperature of liquid and the pool or free stream temperature $T_{sat} - T_\infty$,

ΔT_w = difference between the wall temperature and the saturation temperature of the liquid $T_w - T_{sat}$,

β_f = coefficient of thermal expansion of liquid phase (1/K),

ρ_g = density of saturated vapor (kg/m^3),

ρ_f = density of saturated liquid (kg/m^3),

μ_g = viscosity of saturated vapor ($kg/m \cdot s$),

σ = Stefan-Boltzmann constant.

Equation (5-27) includes the energy transfer by conduction and radiation across the film. The energy transferred by radiation is about 10% of the total energy. The numerical constant in Equation (5-29) would be about 0.5 for natural convection over a sphere with no slip at the surface.

This correlation was developed using spheres of steel, cooper and silver. Experimental results indicate that for particles with an oxide layer on the surface and a low superheat, the Nusselt number may be 80% higher than that for particles with a polished surface.[12] At high superheats, the heat transfer coefficients for oxidized and polished particles converge. Although particles in a debris bed in a nuclear reactor are expected to be oxidized, they may also be very hot, so a multiplier to account for oxidized surfaces is applied.

The surface heat transfer coefficient for film boiling is calculated by the equation

$$h_{sfb} = (Nu)\frac{k_g}{D_p} \tag{5-30}$$

where

h_{sfb} = surface heat transfer coefficient for film boiling ($W/m^2 \cdot K$).

5.3.3 Transition Boiling

In the transition boiling mode of heat transfer, when the debris temperature is between T_{nuc} and T_{TF}, the heat transfer coefficient is calculated by the equation

$$h_{str} = \frac{(T_D - T_{nuc})}{(T_{TF} - T_{nuc})}[h_{sfb} - h_{snuc}] + h_{snuc} \tag{5-31}$$

where

h_{str} = heat transfer coefficient for transition boiling mode of heat transfer ($W/m^2 \cdot K$),

T_{TF} = temperature of debris at which transition boiling heat transfer ends and film boiling heat transfer begins.

The variable T_{TF} is calculated by the equation[3];

$$T_{TF} = 0.16\frac{\rho_g h_{fg}}{k_g}\left[\frac{g(\rho_f - \rho_g)}{(\rho_f + \rho_g)}\right]^{2/3}\left[\frac{\mu_g}{g(\rho_f + \rho_g)}\right]^{1/3}\left[\frac{\sigma}{g(\rho_f + \rho_g)}\right]^{1/2} + T_{sat}. \tag{5-32}$$

5.3.4 Transition from Film Boiling to Convection to Steam

The transition from the film boiling mode of heat transfer to the convection to steam mode of heat transfer is assumed to occur when the void fraction of vapor is between α_4 and 1. The transition from the inverted slug-mist flow regime to the mist flow regime occurs at a void fraction α_4. The equation for calculating α_4 is described in Reference 2. In this range of void fractions, the heat transfer to the liquid and vapor phases are calculated by the equations

$$Q_{cf} = (1 - W_{fg})A_s h_{sfb}(T_D - T_{sat}) \tag{5-33}$$

$$Q_{cg} = W_{fg} Q_{conv}$$

where

Q_{cf} = total heat transfer to liquid phase by convection (W/m^3),

Q_{cg} = total heat transfer to vapor phase by convection (W/m^3),

W_{fg} = weighting function as defined below,

Q_{conv} = heat transfer to vapor as calculated by Equation (5-7) of Section 5.1 (W/m^3).

The weighting function is[12]

$$W_{fg} = y^2(3-2y) \tag{5-34}$$

where

W_{fg} = weighting function for interpolation between film boiling and convection to vapor modes of heat transfer,

y = $\frac{\alpha_g - \alpha_4}{1-\alpha_4}$,

α_g = volume fraction of vapor,

α_4 = void fraction at which flow regime changes from inverted slug-mist flow to mist flow.

5.3.5 Total Heat Transfer to Liquid and Vapor Phases for Two-Phase Flow

The heat transfer to the liquid phase by convection is calculated by the equation

$$Q_{cf} = A_s h_{sf}(T_D - T_{sat}) \tag{5-35}$$

where

Q_{cf} = total heat transfer to liquid phase by convection (W/m^3),

A_s = surface area of particles as calculated by Equation (5-8) for modes other than forced convection to liquid (m^2/m^3). For forced convection to liquid mode, A_s equals 1 (unitless).

h_{sf} = heat transfer coefficient corresponding with the applicable mode of heat transfer, as defined in Table (5-1) for modes other than forced convection to liquid ($W/m^2 \cdot K$). For forced convection to liquid, units of h_{sf} are ($W/m^3 \cdot K$).

The total heat transferred to the fluid is calculated by the equation

$$Q_{tot} = Q_{cf} + Q_{rf} + Q_{cg} + Q_{rg} \tag{5-36}$$

where

Q_{tot} = total heat transferred to the fluid (vapor and liquid phase) (W/m^3). This variable, when multiplied by the volume of a control volume corresponds with the variable Q in the RELAP5 code,

Q_{rf} = total heat transfer to liquid phase by radiation,

Q_{rg} = total heat transfer to vapor phase by radiation.

If the void fraction of vapor is less than α_4, the terms for heat transfer to the vapor in the above equation are equal to zero.

The total heat transferred to the vapor phase is calculated by the equation

$$Q_{totg} = Q_{cg} + Q_{rg} \tag{5-37}$$

where

Q_{totg} = total heat transferred to the vapor phase (W/m^3). This variable, when multiplied by the volume of a control volume, corresponds with the variable QWG in the RELAP5 code. If the void fraction of vapor is less than α_4, this term is equal to zero.

The vapor generation is calculated by the equation

$$\Gamma_w = (Q_{cf} + Q_{rf})/h_{fg} \tag{5-38}$$

where

Γ_w = volumetric vapor generation rate (kg/m^3s). This variable, when multiplied by the volume of porous debris in a control volume and then divided by the fluid volume of the control volume, corresponds with the variable GAMMAW in the RELAP5 code.

5.4 Interphase Heat Transfer

The heat transfer between the liquid and vapor phases of the fluid in porous debris is modeled in an approximate manner. The thermal equilibrium model is used. This model is applied by setting the phasic interfacial heat transfer coefficients to a large value for RELAP5 control volumes that contain porous debris. The suitability of this assumption was assessed by comparing calculated and measured temperatures in an initially hot debris bed that was quenched from the bottom. The temperature history in the debris bed is influenced by the temperature of the steam flowing through the debris bed. Since the calculated and measured temperatures in this region of the debris bed were in generally good agreement, the simplifying assumption of thermal equilibrium of the liquid and vapor phases is appropriate. The assessment results are presented in Section 10.

6. Implementation of Convective Heat Transfer Models into COUPLE

The cooling of porous debris is treated as a heat transfer process that is parallel with the internal heat generation in the porous debris. This treatment is possible because the particles in the porous debris are generally very small compared with the size of a COUPLE node and thus the cooling is uniformly distributed through the node. The effect on debris heatup of convective cooling can be calculated by subtracting the amount of cooling per unit volume of debris from the amount of heat generation per unit volume of debris. Heat transfer by particle to particle conduction is assumed to be negligible at any location where the liquid phase of water is present. The COUPLE code applies the heat generation term in calculating debris heatup as follows;

$$(1-\varepsilon)\rho_D C_D \frac{\partial T}{\partial t} = Q_{net} \tag{6-1}$$

where

ρ_D = density of debris (kg/m^3),

C_D = heat capacity of debris ($J/kg \cdot K$),

ε = porosity of debris,

Q_{net} = net volumetric heat generation rate in debris (W/m^3),

T = temperature of debris (K).

The variable Q_{net} in the above equation is calculated by the equation

$$Q_{net} = Q_D - Q_c \tag{6-2}$$

where

Q_D = volumetric heat generation rate due to decay heat in particles of debris (W/m^3),

Q_c = heat transferred from debris to fluid by convective heat transfer (W/m^3).

The variable Q_c, which is the volumetric rate of removal of heat by convective heat transfer is calculated for every possible regime of heat transfer by the equations presented in Section 5.

Equation (6-1) has omitted the terms for calculating the transport of heat by conduction. This simplification is appropriate when liquid water is present in the interstices of the porous debris, which results in heat transfer by convection dominating over heat transfer by conduction. If liquid water is not present, then the terms for calculating the transport of heat by conduction are included as shown in Equation (2-1).

The implementation of the models for convective heat transfer was accomplished by transforming the COUPLE Fortran variable that stores the volumetric heat generation into a variable that equals the term Q_{net} in Equation (6-2). The Fortran variable transformed is named bg(i), which is the volumetric heat generation (W/m^3) at node i of the COUPLE model mesh. This variable is calculated in subroutine EGEN1. After calculating bg(i) accounting for heat generation, a call is made to the subroutine named HTRC3B to calculate the convective cooling at each node in the COUPLE mesh with debris. The COUPLE model data base was expanded to store the vapor generation rate and the heat transfer to the liquid and vapor phases of the coolant for each COUPLE node. The new variables added to the data base are defined in Table 6-1 and the Fortran changes made to subroutine EGEN1 are described in Table 6-2. A

Table 6-1. Variables added to COUPLE data base for modeling heat transfer to fluid in open porosity.

Fortran variable	Units	Definition
ihpore(n)	-	*indicator of whether n-th convective node has participated in heat transfer from porous debris to fluid, 0=no, 1=yes; it is defined in subroutine egen2 and stored in common block alcm,*
qcrdeb(i)	*W*	*heat removed by convective and radiative heat transfer from debris at node i to fluid in open porosity at node i, array stored in common block alcm,*
iptpor	-	*pointer to location of array ihpore in common block alcm, stored in common block iparm,*
iqcrdb	-	*pointer to location of array qcrdeb in common block alcm, stored in common block iparm,*
ndbthr	-	*indicator of option for modeling of debris to fluid heat transfer, 1=detailed model, 0=simplified model, stored in common block iparm,*
mdbelm (n)	-	*value of first index of debcom arrays for element m,*
ndbelm (n)	-	*value of second index of debcom arrays for element m,*
iptmdb	-	*pointer to mdbelm array,*
iptndb	-	*pointer to ndblm array.*

flow chart was previously shown in Figure 4-1 of the information exchanged in various subroutines in SCDAP/RELAP5 in order to calculate the effect of convective heat transfer on the heatup of the debris.

Input variables are required for subroutine HTRC3B in order to use this subroutine for calculating the heat transfer between porous debris and fluid in the lower head of the reactor vessel. These input variables were added to the common block named debcom. This common block also stores the variables output by subroutine HTRC3B. Table 6-3 lists these input and output variables. The input variables include; (1) porosity of debris, (2) particle size of debris, (3) surface area to volume ratio of debris, (4) volume of debris, (5) temperature of debris, and (6) index of RELAP5 volume within which the debris

Table 6-2. Modifications of subroutine EGEN1 for modeling convective and radiative cooling.

Line of Fortran	Comments	Line status[a]
subroutine egen1(bg,xm2,ng2, . . . # powrat,r, z, tz, pore, dimpe, qcoupl, qwgcou, gamcou, qcrdeb, ir5vec,	*add arguments for variables needed in debris to fluid heat transfer*	*M*
# ihsave, ihpore, mdbelm, ntf2,	*add arguments for variables needed in debris to fluid heat transfer*	*N*
# elem, jelem, elemij, imme, ncslp, ndbthr)	*add arguments for variables needed in debris to fluid heat transfer*	*M*
**in32 ir5vec,ihsave, ihpore*	*adjust for 32 bit integer in 64 bit word*	*M*
**call comctl*	*add parameters needed for RELAP5 volume data block*	*N*
**call voldat*	*RELAP5 volume data block*	*N*
**call fast*	*RELAP5 data*	*N*
**call scddat*	*add common block defining dimension of arrays in common block debcom*	*N*
call debcom	*add debcom common, which contains input and output variables for subroutine htrc3b*	*N*
do 700 n=1,numel	*numel=number of elements*	*N*
i=ix(1,n)	*identify nodes at each corner of element*	*N*
nn=ndbreg+1	*initial value for index nn, which is the second index in the two-dimensional arrays in common block debcom*	*N*
mm=1	*initial value for index mm, which is the first index in the two-dimensional arrays in common block debcom*	*N*
if(pore(n).lt.0.1)go to 700	*skip over node with nonporous debris*	*N*

Table 6-2. Modifications of subroutine EGEN1 for modeling convective and radiative cooling. (continued)

Line of Fortran	Comments	Line status[a]
if(mm.lt.ndax)then	*determine unique set of indices (mm,nn) for couple node i*	*N*
mm=mm+1		*N*
else		*N*
nn=nn+1		*N*
if(nn.gt.ndxbrg)then	*protect against possibility of overflowing dimension of debcom arrays*	*N*
write message		*N*
stop	*stop execution of code*	*N*
end if	*end of "if()then" block on protection*	*N*
end if	*end of "if()then" block on defining mm and nn indices*	*N*
nvoldb(nn)=1	*define one RELAP5 control volume for nn-th debris region*	*N*
ir5=0	*initialization*	*N*
istop=0	*initialization*	*N*
do702ncou=1,ncevr5	*begin do loop to identify RELAP5 volume that node i is connected to*	*N*
ihpore(ncou)=0	*set default value*	*N*
if(istop.eq.1)go to 20	*match already found*	*N*
if(ihsave(ncou).eq.i.and.ntf2(ncou).ge.0)then	*match found*	*N*
ir5=ncou	*store sequence number of convective node*	*N*
ihpore(ncou)=1	*identify that convective node is involved with heat transfer to interstitial fluid*	*N*

Table 6-2. Modifications of subroutine EGEN1 for modeling convective and radiative cooling. (continued)

Line of Fortran	Comments	Line status[a]
istop=1	*indicate that no further searching required to identify sequence number of convective node*	*N*
end if		*N*
702 continue		*N*
if(ir5.eq.0)go to 702	*ir5 = 0 = no porus debris at node*	*N*
numdbv(mm,nn)=ir5vec(ncou)+filndx(4)	*store RELAP5 volume index for debris location (mm,nn)*	*N*
idbvol(ir5vec(ncou)+filndx(4))=2	*identify that porous debris present in RELAP5 control volume*	*N*
mdbvol(ir5vec(ncou)+filndx(4))=mm	*define first index in debcom common block that corresponds with RELAP5 control volume with index of ir5vec(ncou)+filndx(4)*	*N*
ndbvol(ir5vec(ncou)+filndx(4))=nn	*define second index in debcom common block that corresponds with RELAP5 control volume with index of ir5vec(ncou) + filndx(4)*	*N*
tmpdeb(mm,nn)=tz(i)	*define temperature*	*N*
porvol(mm,nn)=pore(n)	*define porosity*	*N*
ddbvol(mm,nn)=dimpe(n)	*define particle size of debris*	*N*
*aovrdb(mm,nn)=(1.-pore(n))*6./dimpe(n)*	*define surface area to volume ratio*	*N*
voldeb(mm,nn)=bv(i)	*define volume of debris*	*N*
call htrc3b(mm, nn)	*(mm, nn) = indices identifying location of debris in framework of SCDAP data base*	*N*
*voldeb=2π *vole(1,n)*	*1=i-th node, 2=k-th node, etc.*	*N*
qcoupl(ir5)=qcoupl(ir5)+qnchdb(mm,nn)	*total heat to RELAP5 volume*	*N*

Table 6-2. Modifications of subroutine EGEN1 for modeling convective and radiative cooling. (continued)

Line of Fortran	Comments	Line status[a]
qwgcou(ir5)=qwgcou(ir5)+qfgdeb(mm,nn)	*heat to vapor phase*	*N*
*gamcou(ir5)=gamcou(ir5)+gmwdeb(mm,nn)*2π *bv(i)/v(numdbv(mm,nn))*	*volumetric vapor generation rate, v=volume of RELAP5 control volume*	*N*
bg(i)=bg(i)-qnchdb(mm,nn)/bv(i)	*adjust power for heat loss, COUPLE nodes map one for one into indices (mm,nn)*	*N*
repeat lines beginning with "ir5=0" and ending with line above for nodes j, k, and l		*N*
a: E = existing line, M = modified line, N = new line		

is located. The output variables are; (1) heat transfer between the debris and fluid, (2) heat transfer between debris and vapor phase of the fluid, and (3) volumetric vapor generation rate.

Table 6-3. Variables in common block debcom that are input and output variables for subroutine HTRC3B for porous debris heat transfer.

Variable name	Units	Category	Variable definition
porvol(m,n)	*unitless*	*input*	*porosity of debris at location defined by indices (m,n)*
ddbvol(m,n)	*m*	*input*	*diameter of debris particles (m)*
aovrdb(m,n)	*(1/m)*	*input*	*surface area of debris per unit volume of debris*
tmpdeb(m,n)	*K*	*input*	*temperature of debris (K)*
voldeb(m,n)	m^3	*input*	*volume of debris*
nvoldb(n)	-	*input*	*number of RELAP5 control volumes in stack of control volumes represented by index n*
numdbv(m,n)	-	*input*	*index of RELAP5 control volume at location (m,n)*
qnchdb(m,n)	*W*	*output*	*rate of heat transfer between debris and fluid.*
qfgdeb(m,n)	*W*	*output*	*rate of heat transfer between debris and vapor phase of coolant*
gmwdeb(m,n)	$(kg/m^3.s)$	*output*	*volumetric vapor generation rate*

The input and output variables in common block debcom are defined for each SCDAP and COUPLE node with porous debris. The node locations are identified by indices that define the radial and axial position of the debris. For in-core debris, these indices are mapped according to axial nodes and radial

segments in the core region. For debris represented by the COUPLE model, these indices are mapped as a function of the COUPLE nodes. The indices used for debris represented by the COUPLE model will not overlap those used for in-core debris. In order to conserve computer memory, the lower bound of the indices for debris represented by the COUPLE model will be contiguous with the upper bound of the indices used to represent in-core debris. As shown previously, Table 6-2 shows the basic structure of Fortran programming that will be added to subroutine EGEN1 to determine the indices for the debcom common block variables and define the values of the required debcom variables. Subroutine HTRC3B will be modified to have an additional input variable that defines the starting value of the index m in the do500 do loop in this subroutine. This modification is described in Table 6-4. In the call to subroutine HTRC3B from subroutine SCDAD5, the input argument mstart will be defined to have a value of 1. The basic structure of subroutine HTRC3B is described in Table 6-5.

Table 6-4. Fortran modifications to subroutine HTRC3B for porous debris heat transfer.

Line of Fortran	Comments	Status[a]
subroutine htrc3b(mstart, n, # icllhb)	*add mstart and icllhb to argument list, where mstart is starting value of index m, icllhb is indicator of whether HTRC3B is called by SCDAD5 or EGEN1*	*M*
mmax = nvoldb (n) *if (icllhb.eq.2) mmax = mstart*	*set mmax to value appropriate for subroutine calling HTRC3B*	*N*
do 500 m=mstart,mmax	*make starting value of index m a function of input argument instead of always being equal to 1*	*M*
a: M = modified line		

Table 6-5. Basic structure of subroutine HTRC3B for calculating debris to fluid heat transfer.

Line of Fortran	Comments
subroutine htrc3b(mstart, n, icllhb)	*mstart = starting value of index m in do500 do loop*
**call comctl*	*access RELAP5 variables*
**call contrl*	*access RELAP5 variables*
**call voldat*	*access RELAP5 variables*
**call fast*	*access RELAP5 variables*
**call ufiles*	*access RELAP5 variables*

Table 6-5. Basic structure of subroutine HTRC3B for calculating debris to fluid heat transfer. (continued)

Line of Fortran	Comments
iv=ir5vc1+filndx(4)	*index for RELAP5 variables in voldat common block*
block of coding to determine heat transfer regime based on criteria defined in Table 2-1; regime is function of volume fraction of liquid and debris temperature	
block of coding that calculates convective heat transfer for each heat transfer regime according to correlations defined in Section 2,	
block of coding that calculates the heat transferred to liquid and vapor phases by radiation heat transfer	
block of coding that calculates total rate of heat transfer to fluid at the specified location in debris, also total heat transfer to vapor phase of fluid, and volumetric vapor generation rate	
end of subroutine	

The changes made to the argument list of subroutine EGEN1 required changes to the call of subroutine EGEN1 from subroutine COUPLE. These changes are described in Table 6-6.

Table 6-6. Fortran changes in subroutine COUPLE for implementing new models for heat transfer in porous debris.

Line of Fortran	Comments	Status[a]
call egen1(bg, xm2, ng2, ...	*extend call to egen1 to account for variables needed to model heat transfer to fluid*	*E*
# powrat, r, z, tz,, pore, dimpe, qcoupl, qwgcou, ...	*add to call pointers needed for debris to fluid heat transfer*	*M*
# ihsave, ihpore, mdbelm, ndbelm, ntfz	*add to call pointers needed for debris to fluid heat transfer*	*N*
# ielem, jelem, j, imme, ncslp, ndbthr)	"	*N*
a: E = existing line of fortran, M = modified line, N = new line.		

Several subroutines required minor modifications for implementation of porous debris to fluid heat transfer. Subroutine COUPLE had the call to DBVPGN skipped and the variable qd set to zero when the option to use the advanced porous debris heat transfer model is defined by the code user. In subroutine COUQOT after start of the do820 do loop, a statement was added to skip the calculation of qcoupl, qwgcou and gamcou when ihpore(n) (indicator of calculation of debris to fluid heat transfer) is equal to 1. In the do80 do loop of subroutine CG2, the variable ihpore(i) was initialized to zero. In the do10 do loop of subroutine ICPL, the variable qcrdeb(i) was initialized to 0.0. In subroutine RGEN after initialization of variable ipfrto (pointer to multiplier on RELAP5 power density table for each node in COUPLE mesh), the initialization of the variable iqcrdb (pointer to value of heat transfer from debris to fluid) was added in manner parallel to initialization of ipfrto, whereby the additional index is equal to result of incrementing the previous index by the number of nodes in the COUPLE mesh. In subroutine CONSET, the variable iptpor (pointer to array ihpore) was defined in manner parallel to definition of the pointer iptihs (pointer to array ihsave), whereby the additional index is equal to the result of incrementing the previous index by the number of nodes in the COUPLE mesh defined to have convective heat transfer. The common block iparm had the integer variables iqcrdb and iptpor added to it. The indicator of the option to be used for calculating debris to fluid heat transfer (variable ndbthr) was be defined by input in subroutine RCOUPL in the A.21.3 block of data. The subroutine MAJCOU was extended to print for every node with porous debris the ratio of heat transfer to fluid to internal heat generation (qcredeb(i)/bg(i)). For the case of zero power, the printout is not performed. Subroutine RBUNDL was extended to include an input variable that defines for an analysis whether the detailed or simplified debris thermal hydraulic models are to be used.

The heat transfer between the liquid and vapor phases of the fluid in porous debris is modeled in an approximate manner. The thermal equilibrium model is used. The thermal equilibrium model is employed by setting the interfacial heat transfer coefficient to a high value. In particular, the Fortran lines shown in Table 6-7 were added to subroutine PHANTV.

Table 6-7. Fortran lines added to RELAP5 subroutine PHANTV to model interphase heat transfer in porous debris.

Fortran line	Comments	Status[a]
337 continue		*E*
endif		*E*
if(idbvol(i).eq.2) then	*after above two lines, check for possibility of porous debris in RELAP5 volume with index i*	*N*
hif(i)=1.0e+9	*set interfacial heat transfer coefficient to large value*	*N*
hig(i)=1.0e+9	*set interfacial heat transfer coefficient to large value*	*N*
endif		
a: E = existing line, N = new line		

7. Flow Losses and Interphase Drag in Porous Debris

This section describes the extensions made to the modeling of flow losses and interphase drag in porous debris regions in order to more accurately calculate the heatup of the porous debris. The flow losses and interphase drag are a function of the flow regime. First, the algorithm used to identify the flow regime for all possible ranges of coolant conditions is presented. Second, the algorithm used to calculate the flow losses due to contact of the fluid with the debris is described. Third, the algorithm used to calculate interphase drag is described. These algorithms are presented in abbreviated form in this report; a complete description of these algorithms is presented in Reference 2.

7.1 Flow Regime Identification

The flow regime is assumed to be identified by the volume fraction of vapor in the fluid and by the heat transfer regime. The heat transfer regime is determined by the algorithm presented in Section 2. For pre-CHF heat transfer regimes, five flow regimes are assumed to be possible in porous debris. These five regimes are; (1) bubbly flow, (2) bubbly-slug flow, (3) slug flow, (4) slug-annular flow, and (5) annular flow. A schematic of the flow regimes is shown in Figure 7-1. In the figure, "k" is a node number that identifies the location of porous debris. For post-CHF heat transfer regimes, five flow regimes are also identified; (1) inverted annular flow, (2) transition from inverted annular flow to inverted slug flow, (3) inverted slug flow, (4) inverted slug-mist flow, and (5) mist flow. A schematic of these flow regimes is shown in Figure 7-2.

The pre-CHF flow regimes are distinguished by the volume fraction of vapor as defined by the following equations;

Bubbly Flow

$$0 < \alpha_g < \alpha_1 \tag{7-1}$$

where

$$\alpha_1 = \begin{cases} 0.6(1-\gamma)^2 & 1.0 \geq \gamma > 0.29 \\ 0.3 & \gamma \leq 0.29 \end{cases} \quad \text{and}$$

$$\gamma = D_b / D_p, \text{ and}$$

$$D_b = 1.35\left[\frac{\sigma}{g(\rho_f - \rho_g)}\right]^{0.5}$$

where

D_b = bubble diameter (m),

D_p = particle diameter (m),

α_g = volume fraction of vapor in fluid,

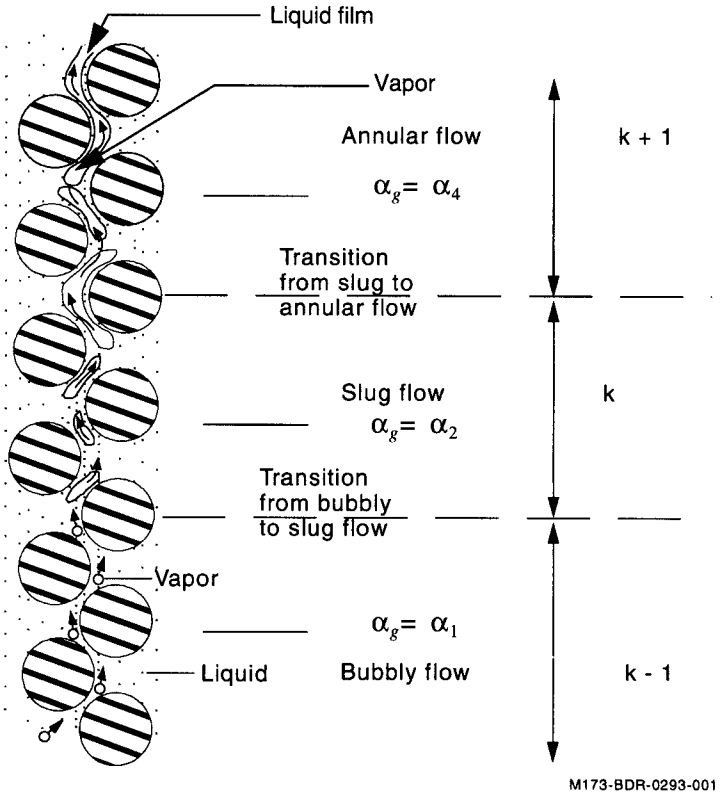

Figure 7-1 Schematic of pre-surface dryout flow regimes.

σ = surface tension (kg/s^2),

g = gravitational acceleration (m/s^2),

ρ_f = density of liquid (kg/m^3),

ρ_g = density of vapor (kg/m^3).

From the fourth assumption listed in Section 4, $\gamma \leq 1$.

Bubbly-Slug Flow

$$\alpha_1 \leq \alpha_g < \alpha_2 \tag{7-2}$$

where

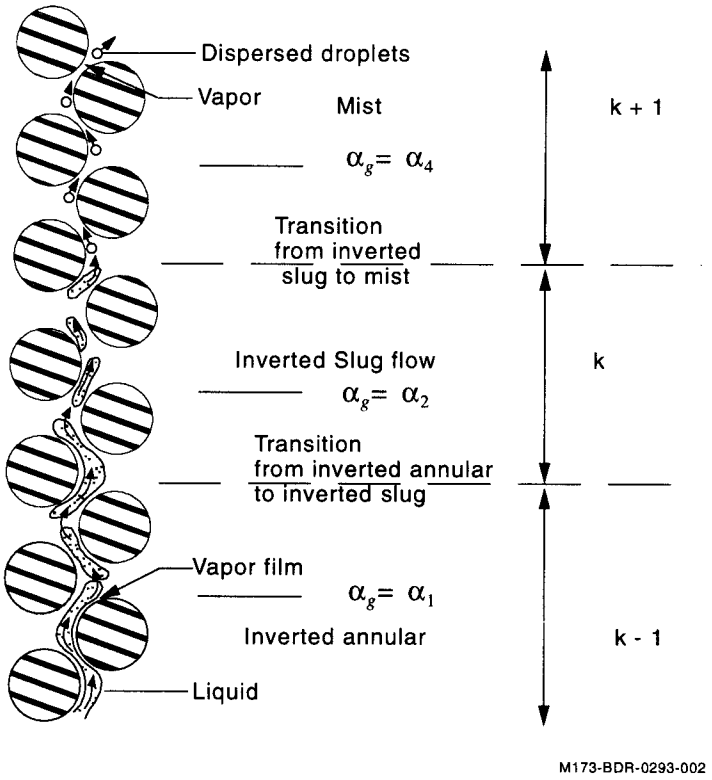

Figure 7-2 .Schematic of post-surface dryout flow regimes.

$\alpha_2 = \pi/6$.

Slug Flow

$$\alpha_2 \leq \alpha_g < \alpha_3 \tag{7-3}$$

where

$\alpha_3 = 0.6$.

Slug-Annular Flow

$$\alpha_3 \leq \alpha_g < \alpha_4 \tag{7-4}$$

where

$\alpha_4 = 0.925$.

Annular Flow

$$\alpha_4 \le \alpha_g \le 1 . \tag{7-5}$$

According to Reference 12, the post-CHF flow regimes are distinguished by the volume fraction of vapor as shown by the following equations;

Inverted Annular Flow

$$0 < \alpha_g < \alpha_1 \tag{7-6}$$

where α_1 is given in Equation (7-1).

Inverted Annular-Inverted Slug Flow

$$\alpha_1 \le \alpha_g < \alpha_2 \tag{7-7}$$

where $\alpha_2 = \pi/6$.

Inverted Slug Flow

$$\alpha_2 \le \alpha_g < \alpha_3 \tag{7-8}$$

where $\alpha_3 = 0.6$.

Inverted Slug-Mist Flow

$$\alpha_3 \le \alpha_g < \alpha_4 \tag{7-9}$$

where $\alpha_4 = 0.925$.

Mist Flow

$$\alpha_4 \le \alpha_g \le 1 . \tag{7-10}$$

Reference 3 recommends that the post-CHF flow regime be distinguished by three thresholds for void fraction, namely α_1, α_2 and α_3. For $\alpha_1 \le \alpha_g < \alpha_2$, the flow regime is inverted annular flow. For $\alpha_2 \le \alpha_g < \alpha_3$, the flow regime is inverted slug flow. For $\alpha_g > \alpha_3$, the flow regime is mist flow. The value of α_1 is approximately given by the equation

$$\alpha_1 = \frac{(1-\varepsilon)}{\varepsilon}\frac{3\delta}{D_p} \tag{7-11}$$

where (7-12)

α_1 = threshold void fraction for inverted annular flow,

ε = porosity of debris,

δ = vapor film thickness (m),

D_p = size of debris particles (m).

Assuming that the liquid field does not contain vapor bubbles and that the debris bed consists of packed spherical particles, the vapor film thickness is related to the volume fraction of vapor by the equation

$$[0.5D_p + \delta]^3 = 0.125D_p^3\,(0.91\alpha_g + 1)$$

The values of α_2 and α_3 were determined empirically. The value of α_3 was defined to be 0.925 and the value of α_2 was defined to be $\alpha_1 + 0.5(\alpha_3 - \alpha_1)$.

The latter of the two methods presented for distinguishing post-CHF flow regimes was implemented.

7.2 Models for Flow Losses

The resistance applied to the flow of liquid and vapor phases of the fluid due to contact with the debris and with each other is a function of the flow regime and velocities of the liquid and vapor phases.[12,14,20] The forces in a two-phase flow in a unit volume cell representing cross-sectionally averaged flow conditions are show in Figure 7-3 Even though only the annular flow configuration is shown, the force balances obtained should be equally applicable to other flow regime. In the figure, F_{pg} represents the drag force by particles on the gas through the liquid layer. F_{pf} is the drag force by particles on the liquid due to liquid motion. F_i is the drag force by liquid on the gas due to relative motion. The flow losses are calculated in terms of drag force (pressure loss gradient) in the porous debris. In the equations below, this drag force is represented by the terms F_{pg} and F_{pf} for the vapor and liquid phases of the fluid, respectively. These terms have the units of N/m^3.

7.2.1 Drag Force for Superheated Steam (Single-Phase).

The gas-phase drag force can be calculated from the Kozeny-Carman equation,[12] which can be written as

$$F_{pg} = \varepsilon[a\mu_g j_g + b\rho_g j_g^2] \tag{7-13}$$

where

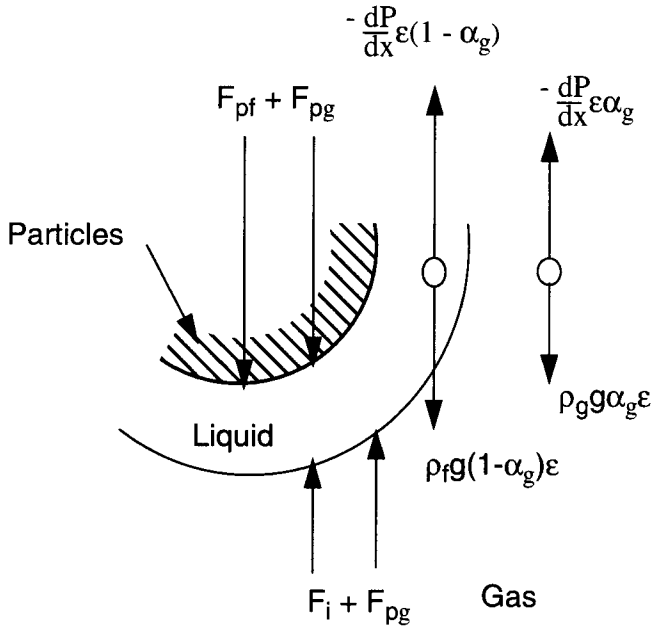

Figure 7-3 .Forces acting in two-phase fluid.

a = viscous coefficient,

$$a = 150\frac{(1-\varepsilon)^2}{\varepsilon^3 D_p^2},$$

b = inertial coefficient,

$$b = 1.75\frac{(1-\varepsilon)}{\varepsilon^3 D_p},$$

F_{pg} = flow resistance (N/m^3),

j_g = superficial velocity of the gas (m/s),

ρ_g = density of the vapor (kg/m^3),

μ_g = viscosity of the vapor $(kg/m \cdot s)$,

ε = porosity of debris.

The superficial velocity j_g is related to the velocity of steam in the interstices by the equation;

$$j_g = \varepsilon v_g \tag{7-14}$$

where

v_g = velocity of vapor (m/s), which is calculated by RELAP5.

7.2.2 Drag Force for Subcooled and Saturated Liquid (Single-Phase)

The debris drag force acting on the single-phase is calculated by the equation

$$F_{pf} = \varepsilon[a\mu_f j_f + b\rho_f j_f|j_f|] \tag{7-15}$$

where

j_f = superficial velocity of the liquid (m/s),

ρ_f = density of the liquid (kg/m^3),

μ_f = viscosity of the liquid $(kg/m \cdot s)$.

The superficial velocity j_f is related to the velocity of fluid in the interstices by the equation;

$$j_f = \varepsilon v_f . \tag{7-16}$$

where

v_f = velocity of liquid (m/s), which is calculated by RELAP5.

7.2.3 Drag Force for Two-Phase Flow

The friction between the two phases and the debris can be modeled with two distinct drag components[12], i.e., particle-gas, and particle-liquid. The particle-gas drag force (F_{pg}) is the drag force by the particles on the gas through the liquid layer, which is opposed by an equal and opposite force applied by the particles on the other side of the liquid layer. The particle-liquid drag force (F_{pg}) is the force by particles on the liquid due to liquid motion, i.e., the liquid drag force against the particles due to liquid motion.

7.2.3.1 Particle-Gas Drag Force for Two-Phase Flow

The Kozeny-Carman equation for the particle-gas drag force per unit of total debris bed volume can be written as

$$F_{pg} = \varepsilon\left[\frac{a\mu_g j_g}{k_g} + \frac{b\rho_g j_g^2}{\eta_g}\right] \tag{7-17}$$

where

$$a = 150\frac{(1-\varepsilon)^2}{\varepsilon^3 D_p^2},$$

$$b = 1.75\frac{(1-\varepsilon)}{\varepsilon^3 D_p}.$$

The variables k_g and η_g are the relative permeabilities, which vary with different flow regimes.

The relative permeabilities may be explicitly written as follows.

For Bubbly and Slug Flows

$$k_g = \left(\frac{1-\varepsilon}{1-\varepsilon\alpha_g}\right)^{4/3}\alpha_g^3 \text{ and } \eta_g = \left(\frac{1-\varepsilon}{1-\varepsilon\alpha_g}\right)^{2/3}\alpha_g^3. \tag{7-18}$$

For Slug-Annular Flow

$$k_g = \frac{\left(\left(\frac{1-\varepsilon}{1-\varepsilon\alpha_g}\right)^{4/3}\right)\alpha_g^2}{\left(W + \frac{1-W}{\alpha_g}\right)} \text{ and } \eta_g = \frac{\left(\frac{1-\varepsilon}{1-\varepsilon\alpha_g}\right)^{2/3}\alpha_g^2}{\left(W + \frac{1-W}{\alpha_g}\right)} \tag{7-19}$$

where W is the weighting function written as

$$W = \xi^2(3-2\xi), \text{ and } \xi = \frac{\alpha_g - \alpha_3}{\alpha_4 - \alpha_3}.$$

For Pure Annular Flow

$$k_g = \left(\frac{1-\varepsilon}{1-\varepsilon\alpha_g}\right)^{4/3}\alpha_g^2 \text{ and } \eta_g = \left(\frac{1-\varepsilon}{1-\varepsilon\alpha_g}\right)^{2/3}\alpha_g^2. \tag{7-20}$$

For Inverted Annular Flow, Inverted Annular-Inverted Slug Flow, Inverted Slug Flow, and Mist Flow

The particle-gas drag relationships for these surface-dryout regimes are treated in a similar fashion to the corresponding presurface-dryout regimes except that the roles of vapor and liquid are interchanged.

7.2.3.2 Particle-Liquid Drag Force for Two-Phase Flow

The equation for the particle-liquid drag force per unit of total debris bed volume can be written as

$$F_{pf} = \varepsilon\left[\frac{a\mu_f j_f}{k_f} + \frac{b\rho_f j_f |j_f|}{\eta_f}\right] \tag{7-21}$$

The variables k_f and η_f are the relative permeabilities, which vary with different flow regimes.

For Bubbly, Bubbly-Slug, Slug, Slug-Annular, and Annular Flow

A single expression for the relative permeabilities for these regimes can be written as

$$k_f = \eta_f = (1-\alpha_g)^3 . \tag{7-22}$$

For Inverted Annular Flow

$$k_f = \left(\frac{1-\varepsilon}{1-\varepsilon\alpha_f}\right)^{4/3}\alpha_f^2 \text{ and } \eta_f = \left(\frac{1-\varepsilon}{1-\varepsilon\alpha_f}\right)^{2/3}\alpha_f^2 \tag{7-23}$$

where

α_f = volume fraction of liquid phase.

For Inverted Annular-Inverted Slug Flow

$$k_f = \frac{\left(\frac{1-\varepsilon}{1-\varepsilon\alpha_f}\right)^{4/3}\alpha_f^2}{\left(W + \frac{1-W}{\alpha_g}\right)} \text{ and } \eta_f = \frac{\left(\frac{1-\varepsilon}{1-\varepsilon\alpha_f}\right)^{2/3}\alpha_f^2}{\left(W + \frac{1-W}{\alpha_f}\right)} \tag{7-24}$$

where W is the weighting function written as

$$W = \xi^2(3-2\xi) \text{ and } \xi = \frac{\alpha_f - \alpha_3}{\alpha_4 - \alpha_3}.$$

For Inverted Slug and Mist Flow

$$k_f = \left(\frac{1-\varepsilon}{1-\varepsilon\alpha_f}\right)^{4/3}\alpha_f^3 \text{ and } \eta_f = \left(\frac{1-\varepsilon}{1-\varepsilon\alpha_f}\right)^{2/3}\alpha_f^3 . \tag{7-25}$$

7.3 Models for Interphase Drag

The liquid-gas interfacial drag force (F_i) is the force by the liquid on the gas due to relative motion between the two-phases.

For Bubbly Flow

For the bubbly liquid-gas interfacial drag force, the drag force exerted on a single bubble is multiplied by the number of bubbles per unit volume of the porous layer.

$$F_i = C'_v \frac{\mu_f j_s}{D_b^2} + C'_i \frac{(\rho_f - \alpha_g \rho_f + \alpha_g \rho_g) j_s^2}{D_b^2 \varepsilon} \tag{7-26}$$

where j_s is the drift velocity of the bubble relative to the mixture written as

$$j_s = j_g \frac{(1-\alpha_g)}{\alpha_g} - j_f$$

and the coefficients C'_v and C'_i are expressed as

$$\left.\begin{aligned} C'_v &= 18\alpha_g f \\ C'_i &= 0.34(1-\alpha_g)^3 \alpha_g f^2 \end{aligned}\right\} \text{ for } 0 < \alpha_g \le \alpha_0$$

$$\left.\begin{aligned} C'_v &= 18(\alpha_0 f + \alpha_g - \alpha_0) \\ C'_i &= 0.34(1-\alpha_g)^3 (\alpha_0 f^2 + \alpha_g - \alpha_0) \end{aligned}\right\} \text{ for } \alpha_o \le \alpha_g \le \alpha_1$$

where α_1 is defined by Equation (7-1) and α_0 is the void fraction corresponding to the maximum number of bubbles supported by the surface of the particles. This can be expressed as

$$\alpha_0 = \frac{\pi(1-\varepsilon)}{3\varepsilon} \gamma(1+\gamma)[6\eta - 5(1+\gamma)] \text{ for } \alpha_0 \ge 0.$$

In the above equation,

$$\gamma = D_b / D_p \text{ , and } \eta = \left[\frac{\pi\sqrt{2}}{6(1-\varepsilon)}\right]^{1/3}.$$

The geometric factor, f, is given by

$$f = \frac{1}{2}(1+\gamma) ln\left(1 + \frac{2}{\gamma}\right). \tag{7-27}$$

For Bubbly-Slug Flow

Slugs are considered as long, thin ellipsoids whose lateral dimension is D_b and length is L_b (=$8D_b$). The drag force acting on the bubbly-slug flow regime can be expressed by Equation (7-26), with a smooth

transition between bubbly and slug flow, by using a weighting function for the coefficients. The coefficients are modified as follows.

$$C'_v = 18(\alpha_0 f + \alpha_g - \alpha_0)(1 - W) + 5.21\alpha_g W$$
$$C'_i = (1 - \alpha_g)^3\{0.34(\alpha_0 f^2 + \alpha_g - \alpha_0)(1 - W) + 0.92\alpha_g W\} \quad (7\text{-}28)$$

where

$$W = \xi^2(3 - 2\xi) \text{ and } \xi = \frac{\alpha_g - \alpha_1}{\alpha_2 - \alpha_1}.$$

For Slug Flow

Since the slugs are fairly long and extend beyond a pore length, they do not flow along the particles as do the spherical bubbles at void fractions less than α_0. Thus, a geometrical correction on j_s is not needed. The drag force can be expressed by Equation (7-26) with modified coefficients C'_v, C'_i, which can be written as

$$C'_v = 5.21\alpha_g \text{ and } C'_i = 0.92(1 - \alpha_g)^3\alpha_g.$$

For Slug-Annular Flow

For the transition from slug to annular flow regime, the weighting function defined for particle-gas drag force can be written as

$$F_i = \left[5.21\alpha_g \frac{\mu_f(1 - W)}{D_b^2} + \frac{\varepsilon a \mu_g}{k_g} W\right] j_s \quad (7\text{-}29)$$

$$+ \left[0.92\alpha_g(1 - \alpha_g)^3 \frac{(\rho_f - \rho_f\alpha_g + \rho_g\alpha_g)(1 - W)}{\varepsilon D_b} + \frac{\varepsilon\alpha_g}{1 - \alpha_g} \frac{b\rho_g}{\eta_g} W\right] j_s^2$$

where k_g, η_g and W are defined as for Equation (7-19) and "a" is defined as for Equation (7-17).

For Annular Flow

In annular flow, the reference velocity must be modified to account for the slip between the two phases.

$$F_i = \frac{\varepsilon a \mu_g}{k_g} j_s + \frac{\varepsilon\alpha_g}{1 - \alpha_g}\left(\frac{b\rho_g}{\eta_g}\right) j_s^2 \quad (7\text{-}30)$$

where k_g and η_g are given by Equation (7-20).

For Inverted Annular Flow, Inverted Annular-Inverted Slug Flow, Inverted Slug Flow, and Mist Flow

The interface drag relationships for these post-dryout regimes is treated in a similar fashion to the corresponding pre-dryout regimes except that the roles of vapor and liquid are interchanged.

8. Implementation of Models for Flow Losses and Interphase Drag

The momentum losses and gains to the fluid flowing through porous debris will be represented by the HLOSSF and HLOSSG terms[11,14] in the RELAP5 field equations. These terms are designed to account for momentum losses due to expansions or contractions of flow areas. The momentum losses of fluid flowing through porous debris in the core region will be taken into account by these terms.

The RELAP5 term for HLOSSG is calculated by the equation;

$$HLOSSG = 0.5K_{Lg}v_g \tag{8-1}$$

where

HLOSSG = form or frictional losses (m/s),

v_g = velocity of the vapor phase (m/s),

K_{Lg} = loss coefficient corresponding with velocity v_g (unitless).

The RELAP5 term HLOSSF is calculated in a parallel manner.

For the gas phase, the loss coefficient is related to the term F_{pg} in Section 7.2 as

$$0.5\varepsilon K_{Lg}\alpha_g\rho_g v_g^2 = F_{pg}\Delta x \tag{8-2}$$

where

Δx = distance (m) that fluid flows the distance at velocity of v_g (N/m^2)

Solving the above equation for K_{Lg}, the result is

$$K_{Lg} = \frac{2\Delta x F_{pg}}{\varepsilon\alpha_g\rho_g v_g^2}. \tag{8-3}$$

The loss coefficients for the vapor phase are stored in the RELAP5 variable formgj(i), where "i" is the junction index. The variable formgj(i) is calculated in subroutine HLOSS. For junctions that are connected with control volumes containing porous debris, Fortran coding was added to subroutine HLOSS that calculates formgj(i) by the equation

$$formgj(i) = K_{Lg} = \frac{2\Delta x F_{pg}}{\varepsilon\alpha_g\rho_g v_g^2} \tag{8-4}$$

The term F_{pg} is from Section 7.2. For the single phase case, $\alpha_g = 1$. In calculating formgj(i), Δx is the distance of flow through porous debris represented by junction "i", and ρ_g and v_g are the vapor density and vapor velocity at the junction, respectively.

The loss coefficients for the liquid phase are calculated in a manner parallel to that for the vapor phase. They are stored in the RELAP5 variable formfj(i), which is calculated by the equation

$$formfj(i)) = K_{Lf} = \frac{2\Delta x F_{pf}}{\varepsilon \alpha_f \rho_f v_f^2}. \qquad (8\text{-}5)$$

The term F_{pf} is from Section 7.2. For this single phase case, $\alpha_f = 1$.

The value of formfj(i) is constrained to a maximum value of 250. The results of a sensitivity study of the application of this constraint are presented in the assessment section of this report. The results indicated that the calculation of the transient temperature distribution in a debris bed is not sensitive to the constraint applied to the value of formfj(i).

This implementation of form fj(i) and formgj(i) into the RELAP5 momentum equations is consistent with the current implementation of other such losses, i.e., a partially implicit method is used where v_g^2 is implemented as $v_g^n v_g^{n+1}$ and v_f^2 is implemented as $v_f^n v_f^{n+1}$.

A branch was put into the first part of the do 2000 loop in subroutine HLOSS to calculate formfj(i) and formgj(i) for RELAP5 junctions that represent flow through porous debris regions. The basic structure of the Fortran changes is shown in Table 8-1.

Table 8-1. Modification of subroutine HLOSS for modeling of flow losses in porous debris.

Fortran coding	Comments	Line status[a]
**call voldat*	*RELAP5 volume variable*	*E*
**call scddat*	*after above line, add common block storing length of arrays storing debris indices and characteristics*	*N*
**call debcom*	*add common block storing debris indices and characteristics*	*N*
**call tblsp*	*add common block storing debris indices and characteristics*	*N*
do 2000 m = 1,lvptr(i1)	*start of do2000 loop*	*E*
. . .. . .	*skip display of some lines*	*E*
kx = k + iand(ishft(jcex(i),-13),3)	*kx = index of RELAP5 volume connected to junction i, after adjusting for flow direction, kx is replaced with ky*	*E*

Table 8-1. Modification of subroutine HLOSS for modeling of flow losses in porous debris. (continued)

Fortran coding	Comments	Line status[a]
lx = l + iand(ishft(jcex(i),-10),3)	*lx = index of another RELAP5 volume connected to junction i, after adjusting for flow direction, lx is replaced with ly*	*E*
if (vf.lt. 0.0) then	*beginning of "if()then" block*	*E*
. . .	*contents of "if()then" block*	*E*
endif	*end of "if()then" block*	*E*
if(idbvol(ky).eq.2)then	*check to see whether junction connected with volume containing porous debris, idbvol(ky)=2=yes, place this and following lines immediately after above "if()then" block*	*N*
epsdb=porvol(mdbvol(ky),ndbvol(ky))	*epsdb = porosity of debris*	*N*
diadb=ddbvol(mdbvol(ky),ndbvol(ky))	*diadb = diameter of debris particles (m)*	*N*
velgdb=abs(velgj(i))	*velgj(i) = velocity of vapor phase at junction with index i (m/s)*	*N*
velfdb=abs(velfj(i))	*velfj(i) = velocity of liquid phase at junction with index i (m/s)*	*N*
fpg=f1(epsdb,diadb,velgdb,voidf(ky),rhog(ky))	*fpg=drag force exerted by particles on vapor phase (N/m^3), calculated using correlations described in Section 7.*	*N*
fi=f2(epsdb,diadb,velgdb,voidf(ky),rhog(ky))	*fi=drag force exerted by liquid phase on vapor, calculated using correlations described in Section 7.*	*N*
formgj(i)=formgj(i)+dl(ky)(fpg)/ (epsdb*voidg(ky)*rhog(ky)*velgdb**2)*	*calculate form loss for vapor phase for junction i accounting for presence of porous debris (unitless)*	*N*
fpf=f3(epsdb,diadb,velfdb,voidf(ky),rhog(ky))	*fpf=drag force exerted by particles on liquid phase (N/m^3), calculated using correlations described in Section 7*	*N*
formfj(i)=formfj(i)+dl(ky)(fpf)/ (epsdb*voidf(ky)*rhof(ky)*velfdb**2)*	*calculate form loss for liquid phase for junction i accounting for presence of porous debris (unitless)*	*N*
end if	*end of "if(idbvol(ky).eq.2)then" block*	*N*

Table 8-1. Modification of subroutine HLOSS for modeling of flow losses in porous debris. (continued)

Fortran coding	Comments	Line status[a]
. . .	*repeat for connecting volume with index ly the sequence of coding beginning with line "if(idbvol(ky).eq.2)then" and ending with line "formfj(i)=formfj(i)+dl(ky)*(fpf)/ (epsdb*voidf(ky)*rhof(ky)*velfdb**2)"*	*N*
if(idbvol(ky).eq.2.or.idbvol(ly).eq.2)then	*limit formgj(i) and formfj(i) to upper bound values for porous debris and then go to end of do loop*	*N*
go to 2000	*skip over coding in do loop for volumes without porous debris*	*N*
end if	*end if*	
a: E = existing line, M = modified line, N = new line		

Since the variables formfj(i) and formgj(i) account for wall friction, the RELAP5 variables for wall friction are not needed. The RELAP5 variables in the field equations for wall friction for the liquid and vapor phases are named FWF and FWG, respectively. To preclude a redundant calculation of wall friction, the RELAP5 Fortran variables fwalfj(i) and fwalgj(i) are set to zero in subroutine FWDRAG for junctions connected with control volumes that contain porous debris.

9. Extensions to In-Core Porous Debris

The models implemented for calculating the cooling of porous debris in the lower head are also applicable for calculating the cooling of debris in the core region. Only a moderate amount of extra effort was required to implement these models for in-core debris. A few lines in subroutine SCDAD5 were changed as indicated in Table 9-1.

Table 9-1. Modifications of subroutine SCDAD5 for application of detailed models for cooling of porous debris

line of fortran	comments	status[a]
$if -def,debth	*line to be removed*	*R*
idbvol(l) = 2	*previous line had "idbvol(l) = 1"*	*M*
m =1, icllhb = 1	*place just before line shown below*	*N*
call htrc3b(m, n, icllhb)	*previous line had "call htrc3b(n)"*	*M*
a: E= existing line, N = new line, M = modified line, R = line to be removed		

10. Assessment of Implemented Models

The models for thermal hydraulic behavior in porous debris were assessed by comparisons of SCDAP/RELAP5 calculated behavior of debris with that evaluated by measurements and other benchmarked models presented in the literature.The models for flow loss were assessed by comparing the pressure drop calculated by SCDAP/RELAP5 with that calculated by a benchmarked pressure drop model. The models for heat transfer were assessed by comparing calculated and measured temperatures for the case of reflood from the bottom of an initially hot debris bed. The implementation of the porous debris thermal hydraulic models into the COUPLE model was assessed by evaluating the behavior calculated for a flooded porous debris bed located in the lower head of a reactor vessel.

The assessment problems for pressure drop involved the steady state analyses of the coolant conditions in a porous debris bed with forced flow at the bottom boundary of the debris bed. A schematic of the system analyzed is shown in Figure 10-1.. The assessment was performed for the following coolant

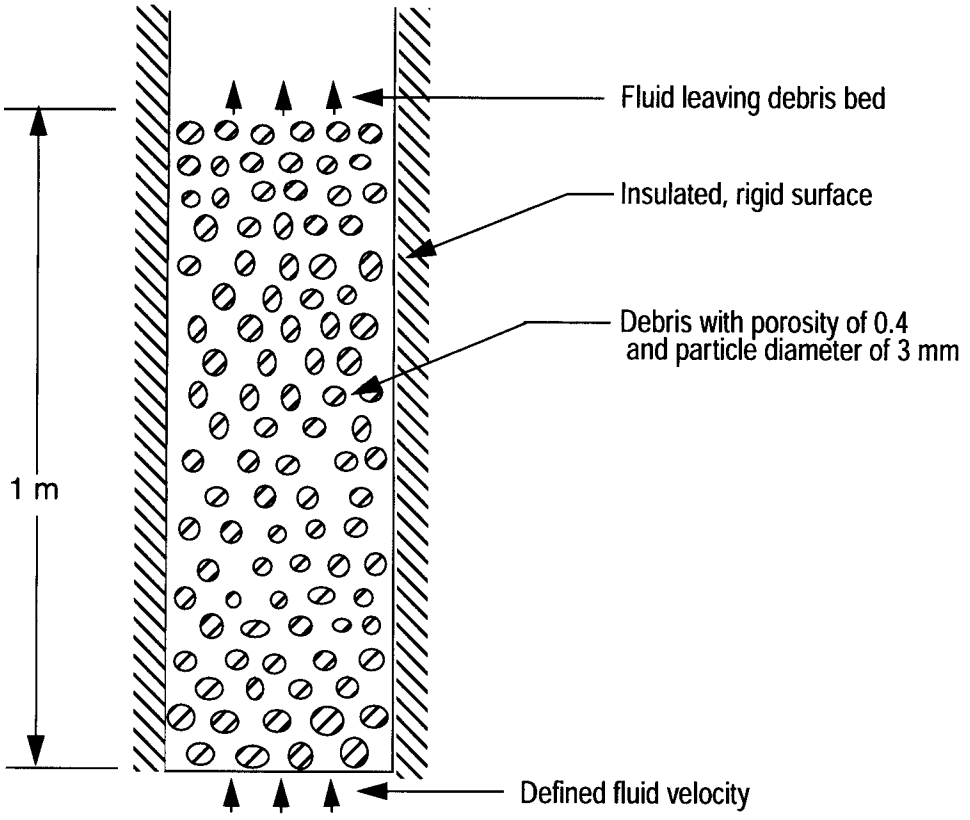

Figure 10-1. Schematic of debris bed analyzed for assessment of flow loss calculations.

conditions; (1) superheated steam, (2) subcooled liquid, and (3) two-phase water. The third case analyzes a debris bed representative of a debris bed resulting from a severe accident in a LWR.[21] The debris and coolant conditions for the three cases are described in Table 10-1.

Table 10-1 . Characteristics of debris bed and coolant conditions for assessment of pressure drop calculations.

Parameter	Case		
	steam	**subcooled**	**two-phase**
porosity of debris	*0.4*	*0.4*	*0.4*
size of particles in debris bed (mm)	*3.0*	*3.0*	*3.0*
height of debris bed (m)	*1.0*	*1.0*	*1.0*
heat generation in debris bed (MW/m^3)	*0*	*0*	*7.5*
coolant pressure (Mpa)	*6.9*	*6.9*	*6.9*
superficial velocity of fluid at bottom of debris bed (m/s)	*0.132*	*$1.39x10^{-2}$*	*$1.47x10^{-2}$*
temperature of fluid at bottom of debris bed (K)	*1050*	*400*	*558.*
quality of fluid at bottom of debris bed	*1.0*	*0.0*	*0.0*
density of heaviest phase of fluid (kg/m^3)	*15.2*	*940.7*	*740*
hydrostatic head (Pa)	*149*	*$9.22x10^3$*	*$3.4x10^3$*

For all three cases, two boundary conditions were defined. The first boundary condition was the velocity of the fluid at the bottom of the debris bed. The second boundary condition was the temperature and quality of the fluid at the bottom of the debris bed. The heat generation in the debris bed was defined to be zero for the two cases involving single-phase coolant and was defined to be 7.5 MW/m^3 for the two-phase fluid case. The nodalization diagram for the analyses is shown in Figure 10-2.. For each case, the debris bed was divided into ten nodes and the fluid in the debris was represented by a stack of ten RELAP5 control volumes. The calculation of the flow losses in porous debris was assessed by comparing SCDAP/RELAP5 calculated pressure drops with independent calculations published in the literature.[12,21]

The assessment of the modeling of flow losses showed that the SCDAP/RELAP5 is correctly calculating the flow losses in porous debris. The SCDAP/RELAP5 flow losses for the three cases identified in Table 10-1 and those presented in the literature for the corresponding cases are compared in Table 10-2. The SCDAP/RELAP5 calculated flow losses are in approximate agreement with the values presented in the literature.

The modeling of heat transfer in porous debris was assessed using the results of a BNL debris experiment involving the quenching from the bottom of a hot porous debris bed.[24] During this experiment, the transient temperature distribution in the debris bed was measured. Since the transient temperature distribution is a function of the flow losses in the debris bed, this experiment in an indirect manner also assessed the modeling of flow losses. A schematic of the experiment is shown in Figure 10-3. Except for representing the fluid in the debris bed by a stack of twelve instead of ten RELAP5 control volumes, the nodalization for the experiment is as shown in Figure 10-2. Each RELAP5 control volume represented a

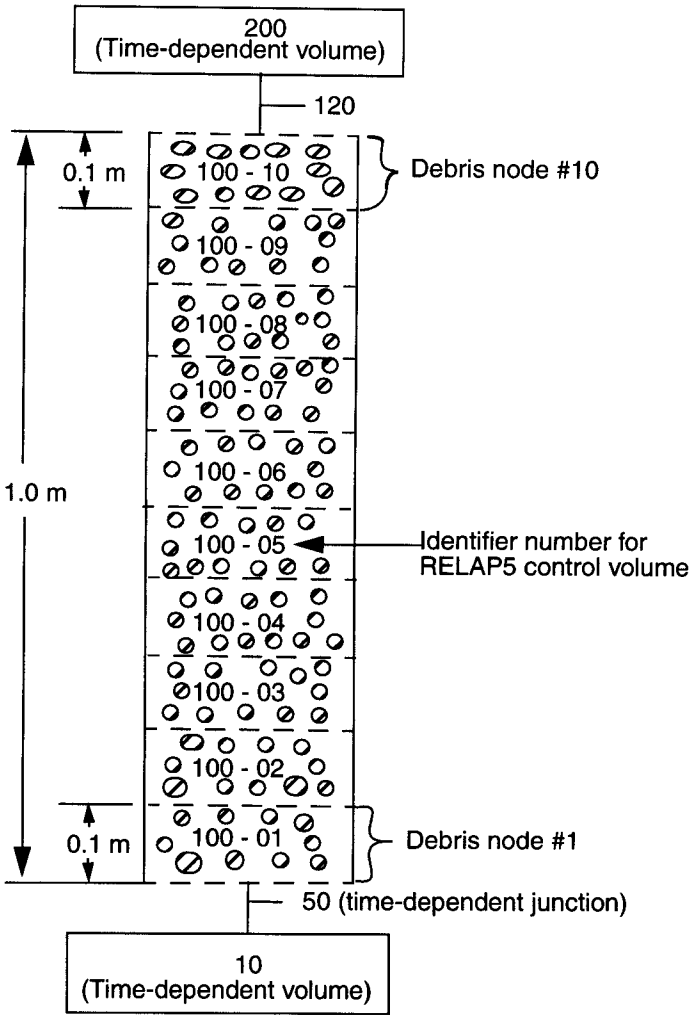

Figure 10-2. Nodalization of debris bed analyzed for assessment of flow loss calculations.

Table 10-2. Comparisons of SCDAP/RELAP5 calculated flow losses with those presented in literature for corresponding cases.

Case	Pressure drop due to flow losses (Pa)	
	SCDAP/RELAP5	**Literature**
superheated steam	1.03×10^3	1.14×10^3
subcooled liquid	1.00×10^3	1.28×10^3
two-phase water	13.5×10^3	12.6×10^3

segment of the debris bed that was 35 mm in height. A summary description of the experiment is shown in Table 10-3.

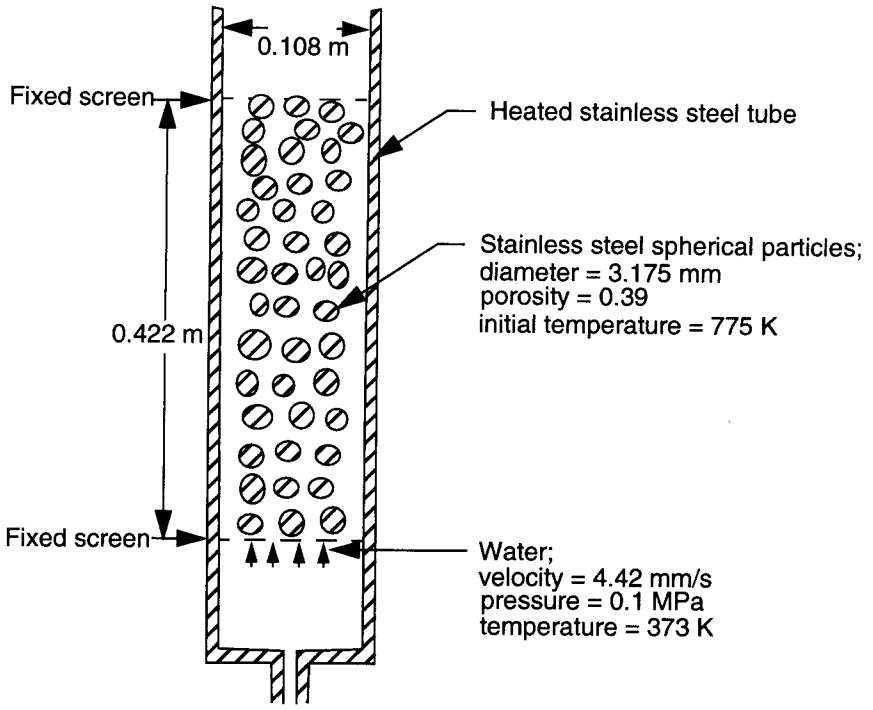

Figure 10-3. Schematic of BNL quenching experiment.

Table 10-3. Summary description of BNL quenching experiment.

Parameter	Value
Porosity of debris	*0.39*
Composition of particles in debris bed	*stainless steel*
Diameter of particles in debris bed (mm)	*3.175*
Height of debris bed (m)	*0.422*
Diameter of debris bed (m)	*0.108*
Initial temperature of debris bed (K)	*775*
Coolant	*water*
Temperature of coolant at bottom of debris bed (K)	*373*
Quality of coolant at bottom of debris bed	*0.0*
System pressure (MPa)	*0.1*
Superficial velocity of coolant at bottom of debris bed (mm/s)	*4.42*

The calculated transient temperatures at two different elevations along the centerline of the debris bed were in general agreement with the measured transient temperatures. The calculated and measured

transient temperatures for the two elevations are compared in Figure 10-4. The elevation of 0.025 m is near the bottom of the debris bed, where reflood began, and the elevation of 0.241 is slightly above the midplane of the debris bed. The debris bed was calculated to quench somewhat quicker than measured. This discrepancy may in part be due to an underprediction of the drag force on the liquid phase of the coolant and in part due to two-dimensional hydrodynamic behavior induced by the wall at the boundary of the debris bed. The overprediction of the temperature at the 0.24 m elevation in the period from 40 s to 50 s is considered due to two-dimensional hydrodynamic behavior, wherein the liquid phase moved up along the wall, formed a pool at the top, and then some of the water flowed down the center region of the debris bed.[24] Nevertheless, the calculated and measured trend in quenching are in good agreement.

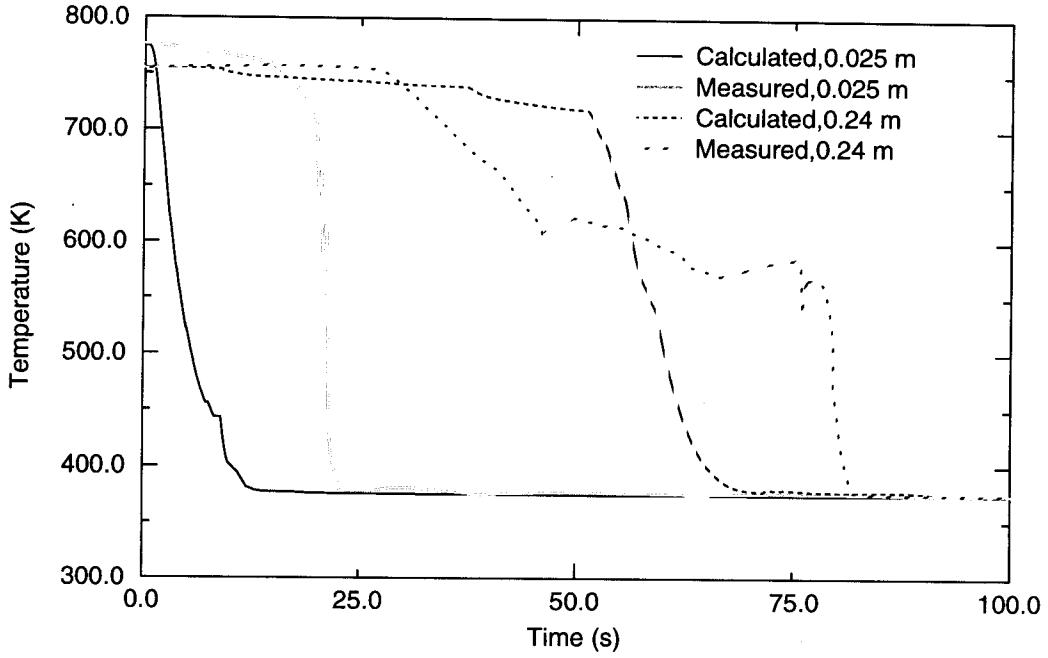

Figure 10-4. Comparison of calculated and measured transient temperature distribution in debris bed

A sensitivity study was performed of the constraint applied to the form loss term for the liquid phase of the coolant. The constraint limits the form loss term to a maximum value of 250; this value is the default value of the constraint on the form loss term for the liquid phase. The sensitivity study consisted of performing two analyses, one of the BNL quenching experiment and the other of the pressure drop in a debris bed with two-phase coolant. In both analyses, the constraint on the form loss term for the liquid state was one hundred times greater than the default value. The results of these two analyses were compared with results obtained with the default value of the constraint. The results for the BNL debris bed quenching experiment are shown in Figure 10-5. The results indicate that the calculation of the transient temperature distribution in the debris bed is not sensitive to a constraint applied to the form loss term for the liquid phase. The effect of the value of a constraint on the form loss term for the two-phase pressure drop problem is shown in Table 10-4. The results show that the case of the constraint being one hundred times greater than the default value results in a considerable overprediction of the pressure drop in a debris bed with two-phase coolant flowing through it. In combining the results of the two analyses performed for a

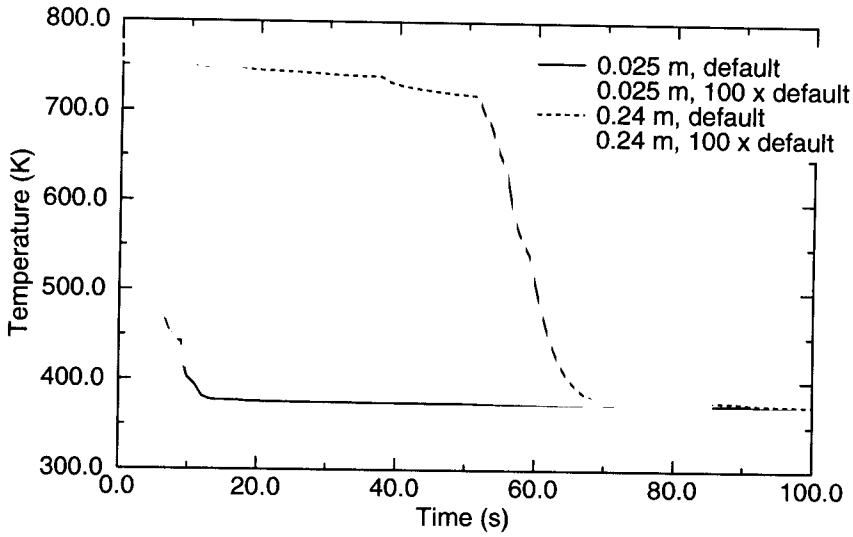

Figure 10-5. Sensitivity of calculated temperature of flooded debris bed to constraint on value of form loss term for liquid phase.

sensitivity study, it is apparent that SCDAP/RELAP5 performs a better analysis of a porous debris bed when the default value of the constraint on the flow loss term for the liquid phase is applied.

Table 10-4. Sensitivity of calculated pressure drop in debris bed with two-phase coolant to constraint on value of form loss term for liquid phase.

Case	Pressure drop (Pa)
literature solution	$12.6x10^3$
SCDAP/RELAP5 with default constraint	$13.5x10^3$
SCDAP/RELAP5 with 100 x default constraint	$10.8x10^4$

The implementation of the porous debris thermal hydraulic models into the COUPLE model was assessed by the analysis of a porous debris bed in the lower head of a reactor vessel A schematic of the system analyzed is shown in Figure 10-6. This figure also shows the COUPLE model nodalization of the porous debris. The porous debris has a total internal heat generation rate of 16.3 MW. The porosity of the debris is 0.4. The debris particles are composed of UO_2. The particles are spherical in shape and have a diameter of 3 mm. The initial temperature of the particles is 600 K. The debris particles slump into the lower head in the 10s interval of time beginning at 11378 s. The RELAP5 nodalization for the analysis is shown in Figure 10-7. At the start of the analysis, the lower head is empty of water. Beginning at the start of the analysis, the lower head is flooded with water at the rate of 80.3 kg/s. The system pressure is 0.2 MPa.

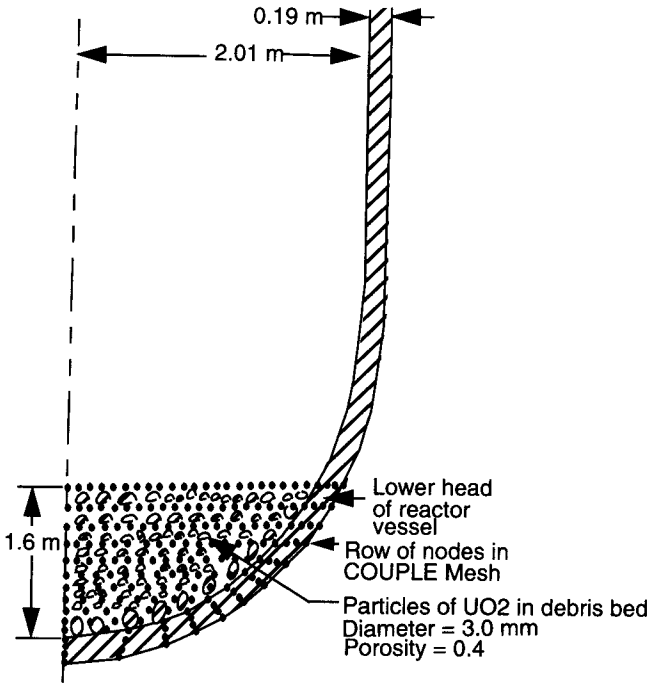

Figure 10-6. Nodalization of debris bed in lower head of reactor vessel.

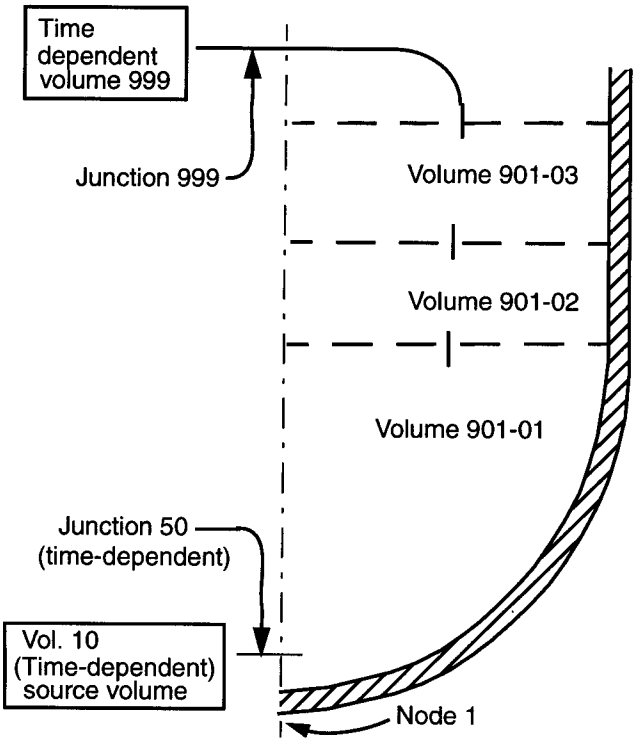

Figure 10-7. RELAP5 nodalization for analysis of porous debris in lower head

An assessment was performed of the energy balance in the debris bed and the coolant that flooded the debris bed. A plot is shown in Figure 10-8 of the transient volume of liquid in the RELAP5 control

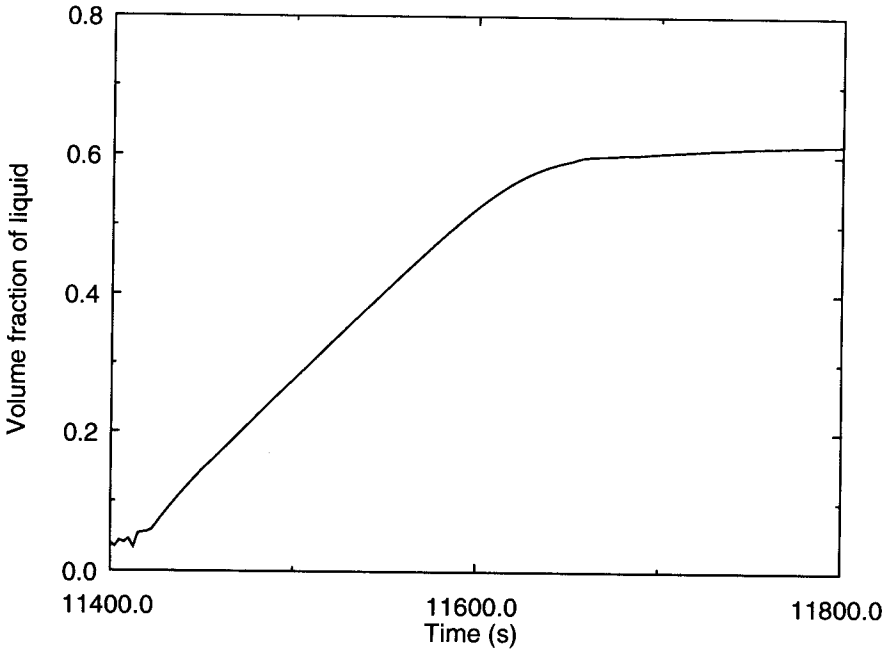

Figure 10-8. Transient volume fraction of liquid in RELAP5 control volume containing the flooded debris bed.

volume containing the flooded debris bed. The volume fraction of liquid increases from 0.0 to 0.5 during the first 200 s of flooding. The transient temperature at the center of the debris bed is shown in Figure 10-9. At this location, the debris cooled in about 200 s from 600 K to a temperature near the saturation temperature of the coolant. The debris bed power and the heat transfer to the coolant are compared in Figure 10-10. After the initial internal energy was removed from the debris, the debris bed power and heat transfer to the coolant converge to the same value. This equality indicates that the COUPLE model for porous debris has been properly interfaced with the RELAP5 model.

Any future assessment of the COUPLE porous debris modeling will involve a much more refined stack of RELAP5 control volumes in the region of the porous debris. This more refined RELAP5 nodalization will permit an assessment of the effect of debris height on the dryout of the debris bed.

In conclusion, SCDAP/RELAP5/MOD3.3 is correctly modeling the flow losses and heat transfer porous debris. The SCDAP/RELAP5 calculated flow losses for three different conditions of coolant were similar to those presented in the literature for corresponding conditions. The SCDAP/RELAP5 calculated transient temperature distribution in a hot debris reflooded from the bottom was similar to the measured transient temperature distribution. The COUPLE model representation of heat transfer in porous debris flooded with water results in a correct energy balance in the overall system analyzed. As a result of the models that have been implemented, SCDAP/RELAP5/MOD3.3 calculates in a more thorough manner the heatup of porus debris in the core region and in the lower head

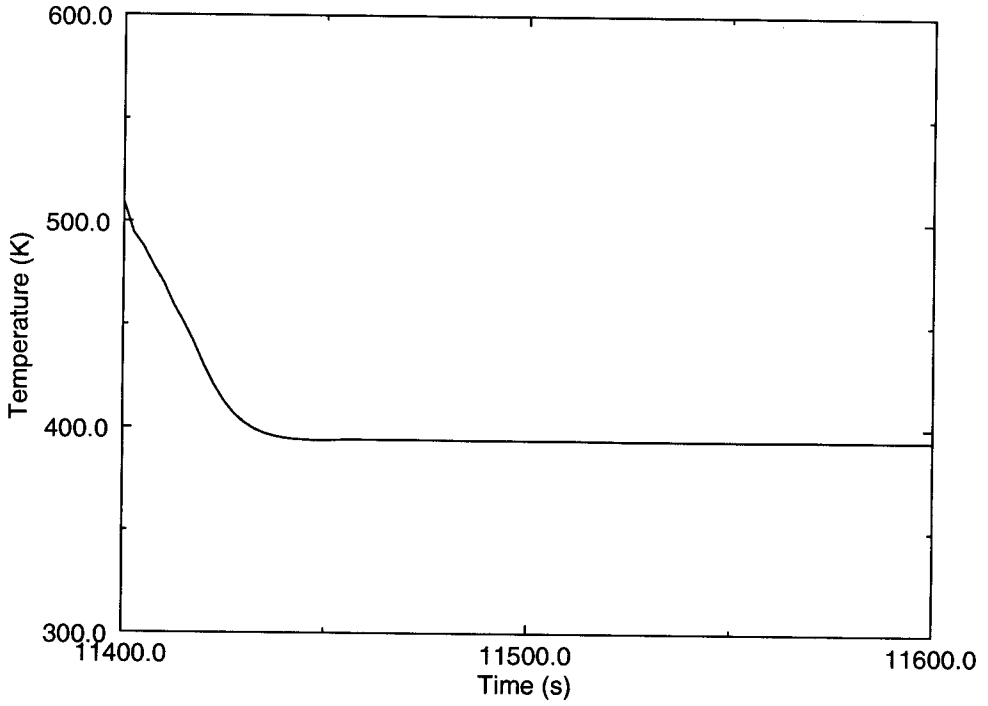

Figure 10-9. Transient temperature at center of debris bed.

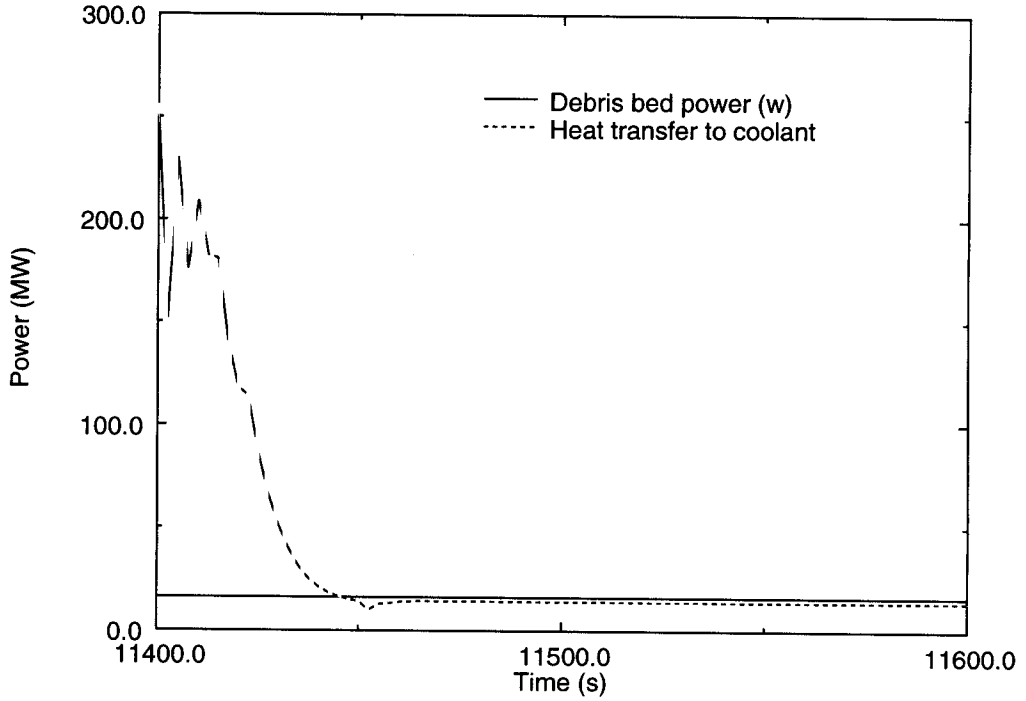

Figure 10-10. Comparison of debris bed power and heat transfer to coolant

11. Summary and Conclusions

Designs were described for calculating the heat transfer and flow losses in porous debris located either in the core region or in the lower head of a reactor vessel. The transient temperature distribution in porous debris in the lower head is calculated by the COUPLE model in the SCDAP/RELAP5/MOD3.3 code. Previously, the COUPLE model had the capability to model convective and radiative heat transfer from the surfaces of nonporous debris in a detailed manner but model only in a simplistic manner the heat transfer and flow losses in porous debris. In order to advance beyond this simplistic modeling, designs were developed for a detailed calculation of heat transfer and flow losses in porous debris and for an accounting of the heat transfer and flow losses in the field equations of the RELAP5 part of the code. The RELAP5 and COUPLE parts of the code were interfaced so that RELAP5 fluid conditions at each node in the COUPLE mesh are transferred to COUPLE for the calculation of the debris temperature distribution and the debris conditions are transferred to RELAP5 for the calculation of fluid conditions within the interstices of the debris.

For the modeling of heat transfer, six modes of convective heat transfer were distinguished and correlations defined for each mode. The six modes of heat transfer were; (1) forced convection to liquid, (2) forced convection to gas, (3) nucleate boiling, (4) transition boiling, (5) film boiling, and (6) transition from film boiling to convection to vapor. Interphase heat transfer was also modeled. The boundaries between the modes of heat transfer were defined as a function of the volume fraction of vapor and the debris temperature. In general, the correlations calculate the rate of convective heat transfer as a function of the local fluid conditions and the local debris porosity, particle size, and temperature.

Designs were also described for models of flow loss and interphase drag in porous debris. These models identified the flow regime and then applied the correlation for flow loss appropriate for that flow regime. The modeling distinguished the following pre-CHF flow regimes; (1) bubbly, (2) bubbly-slug, (3) slug, (4) slug-annular, and (5) annular. The modeling distinguished the following post-CHF flow regimes; (1) inverted annular, (2) inverted annular-inverted slug, (3) inverted slug, (4) inverted slug-mist, and (5) mist. In general, the boundaries between flow regimes were calculated as a function of the volume fraction of vapor and the size of the debris particles. The modeling calculated the particle-gas drag forces and the particle-liquid drag forces for the momentum equations in RELAP5. The modeling also calculated the interphase drag.

The implementation of the models for heat transfer and flow in porous debris involved extensions in computer programming to one subroutine in each of the three major parts of SCDAP/RELAP5/MOD3.3. In the SCDAP part of the code, subroutine HTRC3B was extended. This subroutine calculates convective heat transfer in porous debris as a function of flow regime and the local conditions of the fluid and debris. In the RELAP5 part of the code, subroutine HLOSS was extended. This subroutine calculates flow losses due to geometry change, and was extended to calculate flow losses in porous debris regions. In the COUPLE part of the code, subroutine EGEN1 was extended to identify the RELAP5 control volume overlapping each node in the COUPLE mesh and to call subroutine HTRC3B to obtain the convective heat transfer for each node. Since the models for heat transfer and flow losses in porous debris in the lower head were designed for general application, an extension was designed for the SCDAP subroutine named SCDAD5 to extend the modeling of heat transfer and flow losses in porous debris in the lower head region to the modeling of these variables in porous debris in the core region.

The models for thermal hydraulic behavior in porous debris were assessed by comparisons of SCDAP/RELAP5 calculated behavior of debris with that evaluated by measurements and other benchmarked models presented in the literature. The models for flow loss were assessed by comparing the pressure drop calculated by SCDAP/RELAP5 with that calculated by a benchmarked pressure drop model. These comparisons indicated that the code is correctly calculating the flow losses for fluid conditions ranging from single phase vapor to liquid or two-phase fluid. The models for heat transfer were assessed by comparing calculated and measured temperatures for the case of reflood from the bottom of an initially hot debris bed. With the exception of the calculated timing of quench being somewhat earlier than that measured, these comparisons showed that the calculated transient temperature distribution was in generally good agreement with the measured transient temperature distribution. The implementation of the porous debris thermal hydraulic models into the COUPLE model was assessed by evaluating the behavior calculated for a flooded porous debris bed located in the lower head of a reactor vessel. The evaluation indicated that the interface between the COUPLE and RELAP5 parts of the code was complete.

The models described in this report improve the SCDAP/RELAP5 calculation of the temperature distribution in porous debris resulting from core material slumping to the lower head of a reactor vessel. The models also improve the SCDAP/RELAP5 calculation of the temperature and flow distribution in porous debris which is located in the core region and is flooded by accumulator injection.

12. References

1. The SCDAP/RELAP5 Development Team, "SCDAP/RELAP5/MOD3.2 Code Manual, Volume II: Damage Progression Model Theory," NUREG/CR-6150, Vol. 2, Rev. 1 (INEL-96/0422), July 1998.

2. S. Paik and L. J. Siefken, "Extensions to SCDAP/RELAP5 Code for the Modeling of Thermal-Hydraulic Behavior in Porous Debris Beds - Preliminary Design Report," EGG-RAAM-10683, March 1993.

3. V. K. Dhir, R. Viskanta, and H. Esmaili, "Review of Extensions to SCDAP/RELAP5 Code for the Modeling of Thermal-Hydraulic Behavior in Porous Debris", U. S. Nuclear Regulatory Commission Contract NRC 04 92-045, Task 3, June 1993.

4. E. C. Lemmon, "COUPLE/FLUID: A Two-Dimensional Finite Element Thermal Conduction and Advection Code," EGG-ISD-SCD-80-1, February 1980.

5. J. E. Kelly, J. T. Nitchevek, and M. L. Schway, "Heat Transfer Characteristics of Dry Porous Particular Beds with Internal Heat Generation," Proceedings of ASME/JSME Thermal Engineering Joint Conference, Honolulu, HI, Volume 4, 1983, p. 83.

6. S. Imura and E. Takegoshi, "Effect of Gas Pressure on the Effective Thermal Conductivity of Pack Beds," Heat Transfer Japanese Research, Vol. 3, No. 4, 1974, p. 13.

7. D. Vortmeyer, "Radiation in Packed Solids," 6th International Heat Transfer Conference, Toronto, Canada, 1978.

8. G. P. Wilhite, D. Kunii, and J. M. Smith, "Heat Transfer in Beds of Fine Particles (Heat Transfer Perpendicular to Flow)," AIChE Journal, Vol. 8, No. 3, 1952, p. 340.

9. A. V. Luikov, A. G. Shashkov, L. L. Vasiliev, and Yu E. Fraiman, "Thermal Conductivity of Porous Systems," International Journal of Heat Mass Transfer, Vol. 11, 1968, p. 117.

10. L. J. Siefken et al., "Extension to SCDAP/RELAP5/MOD2 Debris Analysis Models for the Severe Accident Analysis of SRS Reactors, Final Design Report," EGG-EAST-8508, June 1989.

11. The RELAP5 Development Team, "RELAP5/MOD3 Code Manual, Vol. I: Code Structure, System Models, and Solution Methods," NUREG/CR-5535, INEL-95/0174, August 1995.

12. V. X. Tung, "Hydrodynamic and Thermal Aspects of Two-Phase Flow Through Porous Media," Ph. D. Thesis, University of California, Los Angeles, 1988.

13. D. K. Edwards, V. E. Denny and A. Mills, Jr., "Transfer Process", McGraw-Hill Book Comp., New York, New York, 1979.

14. The RELAP5 Development Team, "RELAP5/MOD3 Code Manual, Vol. IV: Models and Correlations," NUREG/CR-5535, INEL-95/0174, August 1995.

15. D. J. Gunn, "Transfer of Heat or Mass to Particles in Fixed and Fluidized Beds," Int. J. Heat and Mass Transfer, Vol. 21, 1978, pp. 467-476.

16. W. M. Rohsenow, "A Method for Correlating Heat Transfer Data for Surface Boiling of Liquids," Trans. ASME, 1952, p. 969.

17. J. S. Ded and J. H. Lienhard, "The Peak Pool Boiling Heat Flux from a Sphere," AIChE Journal, Vol. 18, No. 2, 1972.

18. V. K. Dihr and G. P. Purohit, "Subcooled Film-Boiling Heat Transfer from Spheres," Nuclear Engineering and Design, Vol. 47, 1978, pp.49-66.

19. W. Chu, V. K. Dhir, and J. S. Marshall, "Study of Pressure Drop, Void Fraction and Relative Permeabilities of Two-Phase Flow through Porous Media," AICHE Symposium Series, Vol. 79, No. 225, 1983, pp. 224-235.

20. V. X. Tung and V. K Dhir, "A Hydrodynamic Model for Two-Phase Flow Through Porous Media," Int. J. Multiphase Flow, Vol. 14, No. 1, 1988 pp. 47-65.

21. V. X. Tung, V. K. Dhir, and D. Squarer, "Forced Flow Cooling Studies of Volumetrically Heated Porous Layers," Second International Topical Meeting on Nuclear Reactor Thermal-Hydraulics, Santa Barbara, California, USA, January 11-14, 1983.

22. M. Chung and I. Catton, "Post-Dryout Heat Transfer in a Multi-Dimensional Porous Bed," Nuclear Engineering and Design, 128, 1991, pp. 289-304.

23. I. Catton and M. Chung, "Two-Phase Flow in Porous Media with Phase Change: Post-Dryout Heat Transfer and Steam Injection," Nuclear Engineering and Design, 151, 1994, pp. 185-202.

24. N. K. Tutu et al., "Debris Bed Quenching under Bottom Flood Conditions (In-Vessel Degraded Core Cooling Phenomenology)," NUREG/CR-3850, 1984.

25. C. H. Wang and V. K. Dhir, "An Experimental Investigation of Multidimensional Quenching of a Simulated Core Debris Bed," Nuclear Engineering and Design, 110, 1988, pp. 61-72.